DOE/ET/51013-T

DOE/ET/51013--T243

DE92 002271

Design Study of a 7 kW, Visible Wavelength FEL

Final Report for the year
September, 1989 — August, 1990

Submitted to:

Dr. Charles Primmermann
M.I.T. Lincoln Laboratory

Submitted by:

S.C. Chen
B.G. Danly
R.J. Temkin
J. Wurtele
B. Yang

MIT Plasma Fusion Center

AC02-78ET 51013

DISCLAIMER

CONTENTS

Summary

The M.I.T. Lincoln Laboratory is investigating the possibility of building a free electron laser (FEL) operating at an average power of about 7 kW at wavelengths of 500–600 nm. Additional specifications for the FEL include a bandwidth of less than 0.1 cm^{-1} and a micropulse separation of less than 10 ns. The design study has investigated the basic design parameters of the FEL including an analysis of the electron accelerator, beam line, wiggler and optical cavity. A nonlinear model of the FEL has been used to calculate the FEL gain and efficiency. The required output power appears achievable from an FEL operating at more than 1% efficiency with a conventional RF accelerator. Details of the FEL design are presented in this report which represent the final report for the year from September 1, 1989 to August 31, 1990.

1. Introduction

The M.I.T. Plasma Fusion Center has conducted a study of a visible wavelength, free electron laser (FEL) under subcontract to the M.I.T. Lincoln Laboratory. The purpose of this study was to determine the design parameters and performance of a visible wavelength laser with about 7 kW of average output power. The basic design parameters of the laser were specified by the Lincoln Laboratory Adaptive Optics Group. These parameters included power, wavelength and bandwidth specifications, as described below in Table 1. The present study thus addressed the feasibility of meeting the prescribed design goals with a free electron laser and the basic system design.

The work conducted under this subcontract consisted of three phases. In the first phase, the basic parameters of the free electron laser were established. These parameters included the electron beam energy, current, micropulse length, macropulse length, wiggler design, laser resonator design and preliminary estimates of gain and efficiency.

In phase two, the technology of the FEL system was addressed in some detail. The use of RF linacs of various frequencies, ranging from 0.1 to 3 GHz, was compared. Possible use of a storage ring or other advanced system was also considered. A baseline design of the key accelerator components was carried out with a goal of reliably meeting the design specifications with the minimum cost.

In the third pase of the study, the gain and efficiency of the FEL were estimated using nonlinear FEL codes available at M.I.T. The gain and efficiency were estimated for

different values of peak FEL current, for finite beam quality effects and for different energy spreads. A tapered wiggler system was also investigated with variation in the number of wiggler periods and the rate of wiggler tapering. These studies were able to show that the FEL could achieve an operating efficiency in excess of 1% allowing the goal of 7 kW of time average output power to be achieved. Further studies would be required to demonstrate that the assumed electron beam quality could be achieved in an RF electron linac.

At the end of the present study, an effort was initiated to estimate the bandwidth of the FEL, a critical requirement for applications. This study could not be completed but will be the key goal in the second year of this program.

2. Design of an Optical Wavelength FEL: Overview

2.1 Basic Design Considerations

The M.I.T. Lincoln Laboratory is interested in a free electron laser (FEL) operating at kilowatt power levels and visible wavelengths. This report describes a promising approach for such a FEL and an estimate of the expected performance. Based on this study, M.I.T. Lincoln Laboratory will be able to determine the feasibility of constructing such a FEL.

The M.I.T. Lincoln Laboratory has established a set of specifications for the optical FEL performance. These specifications are listed in Table 1. A detailed discussion of these specifications is contained in a report entitled "Design of an Optical Wavelength FEL" which is contained as Appendix 1 of this report. The major FEL parameters are a wavelength of 500 to 600 nm, a macropulse energy of 7J and a macropulse repetition rate of 1 kHz. The average optical power is 7 kW. These parameters are consistent with present day FEL designs, such as the Boeing FEL. However, no FEL has yet, to our knowledge, actually operated at these average optical power levels. Electron accelerators, which are the major component of the FEL, have operated at average power levels exceeding one megawatt. This indicates that the basic technology of a kilowatt power level FEL is established even though such a FEL has not yet been demonstrated.

The present FEL has two somewhat unusual specifications, namely an optical bandwidth requirement of $\Delta\nu \leq 0.1$ cm^{-1} and a micropulse separation of less than 10 ns. The bandwidth requirement cannot be met by a FEL based on a conventional RF linac. Such

Table 1
Optical FEL Specifications

Wavelength:	$\lambda = 500$ to 600 nm
Pulse Length: (Macropulse)	$\tau_{MP} = 100\mu s$
Pulse Energy: (Macropulse)	$E_{MP} = 7J$
Repetition Rate: (Macropulse)	1 kHz
Laser Bandwidth:	$\Delta\nu \leq 0.1$ cm^{-1}
Laser Power, Macropulse Average	70 kW
Laser Power, Time Average	7 kW
Micropulse Separation	$\leq$ 10 ns

linacs have micropulses of 30 ps or less resulting in a transform limited optical bandwidth that is a factor of at least ten too large (that is, $\Delta\nu > 1$ cm^{-1}). The present report discusses techniques for meeting the optical bandwidth specification of the FEL, such as stretching the electron micropulses from a conventional linac and building a linac with long micropulses, using a storage ring or other approaches.

The micropulse separation of 10 ns or less is also a somewhat unusual requirement. Typical micropulse separations are: 46 ns at Los Alamos (LANL) and 28 ns at Boeing. The use of a short micropulse separation, such as 10 ns, results in a low value of peak current. Since FEL gain increases linearly with current, the resulting FEL design may have too low a gain. This requires a careful analysis of the FEL system to optimize the gain. It may also be possible to build a FEL with a long micropulse separation, such as 80 ns, and to use optical pulse manipulation to decrease the micropulse spacing, as described in the appendix. Our analysis of the FEL gain and efficiency, described in Section 4, indicates that the FEL has greatly improved performance when operated at higher peak currents. This indicates that the FEL design is optimized by maintaining 80 ns separation of the micropulses and using an optical repetition rate multiplier, as described in the appendix, to achieve a 10 ns spacing of the optical micropulses.

2.2 Selection of Preferred Optical FEL Approach

Since the first demonstration of a FEL in the IR region by Elias et al. in 1976 [1], there have been several FEL experiments conducted at optical wavelengths. These are reported elsewhere [2–4] and will not be described here in detail. Furthermore, there have been a series of published design studies of proposed FEL experiments. The insights presented in some of those studies are useful for the present design study.

A FEL working in the optical region, at 648 nm, was reported in 1985 using an electron storage ring, ACO, in Orsay, France [5]. Average output power was less than a milliwatt. The ACO experiment is still active and is being improved, but the possibility of achieving 7 kW of output power from a storage ring FEL is not clear. A second demonstrated approach to visible wavelength FEL emission is a FEL using a linear accelerator. The Stanford superconducting accelerator has operated at 115 MeV and produced 530 nm radiation [6]. The prospects of producing kilowatt output power levels from a superconducting accelerator are not clear. Research on a high average power superconducting accelerator is being conducted for SDIO by TRW. A third demonstrated technology for a visible wavelength FEL is a conventional RF linear accelerator. In 1988, Boeing demonstrated 40

MW of peak power and 2 kW of macropulse average power at a wavelength near 600 nm [7]. These are very encouraging results but the accelerator used produced 16 ps micropulses, much shorter than the 200 ps micropulse length required in the present specifications.

In addition to these three demonstrated approaches, a number of other concepts have been proposed for an optical wavelength FEL. The induction linac FEL has been demonstrated at infrared wavelengths, but it has a short pulse length, 50 ns, and the accelerator is relatively large. The electrostatic FEL cannot operate above about 30 MeV and would require a wiggler with a 0.3 cm period to reach a wavelength of 0.5 μm. Short period wigglers are being studied at many laboratories but have not yet been adequately demonstrated. An additional approach to the FEL is based on the microtron. A visible wavelength FEL is being constructed by a NIST/NRL collaboration [8]. Various compact accelerators, such as recyclotrons, have also be proposed for FEL applications.

Another approach to visible wavelength FEL emission is based on harmonic generation. The emission from the infrared FEL at Stanford has been doubled in nonlinear crystals outside of the laser. The picosecond, high intensity output pulses from the FEL are ideal for this doubling process. However, this may not be feasible at kilowatt power levels. It is also possible to use harmonic emission from the FEL itself, particularly the third harmonic which has relatively high gain in a linearly polarized wiggler.

The use of advanced accelerator technology may also prove important. The long micropulses needed for the present optical FEL may require a novel accelerator, a very low frequency accelerator or an electron pulse stretcher. The use of multiple pass acceleration and energy recovery may also be attractive.

The proposed optical FEL has a very narrow bandwidth requirement, 0.1 cm^{-1}, which is a $(\Delta\lambda/\lambda)$ of 5×10^{-6}. This bandwidth would require transform–limited operation of the FEL device. Several effects can increase the FEL bandwidth. The limited stability of the electron accelerator can cause variation in the electron beam energy, such as chirping during a macropulse or variation in beam energy from one macropulse to another. The arrival time of electron bunches at the FEL oscillator can also vary in time due to jitter in the accelerator. The stability of accelerators is a function of many parameters, depends on the accelerator average power and varies with accelerator type–superconducting, conventional, storage ring, etc. Another major source of increased optical bandwidth is the sideband instability. Sidebands have produced power at wavelengths detuned by 1 to 2% from the central frequency. Recent research at LANL [9] has shown that output at sidebands can be reduced or eliminated by careful tuning of the cavity. Introduction of dispersive elements

into the cavity, such as gratings, has also been tried for sideband suppression. The grating was found to narrow the spectrum but also to reduce the output power.

The bandwidth of the first FEL oscillator experiment at Stanford [10] was 8 nm. Since the emission wavelength was 3.4 μm and the micropulses were only 4 ps long, the observed bandwidth is close to the transform limit. This good result may have been achieved because the accelerator was a superconducting accelerator, which can have high stability. Also, sidebands were absent because the FEL was only just above threshold and sidebands only grow in a regime of strong saturation. In the Boeing FEL burst mode experiments reported in June, 1988, a bandwidth of 3 nm was measured when operating at 0.62 μm wavelength and 8 ps micropulses. Using $\Delta\lambda = \lambda^2\Delta\nu/c$ and $(\Delta\nu)(\Delta t) = 1$, the predicted transform limited bandwidth is 0.16 nm, much lower than the observed value. The Boeing experiment was designed to achieve high power rather than a minimum optical bandwidth, so that the wider bandwidth result is not an accurate predicter of results that could be achieved in an optimized FEL design.

Recent results [11] from the 10 μm FEL experiment at LANL have shown narrow bandwidth emission. Below saturation, the measured bandwidth is $\Delta\lambda/\lambda$ of 0.3% or a width $\Delta\lambda$ of 30 nm. This width is consistent with the transform limit for 10 ps micropulses. Above saturation, the bandwidth increases greatly when sidebands are generated. By careful detuning of the cavity at high power, sidebands are suppressed and narrow bandwidth spectra are achieved, with $\Delta\lambda/\lambda$ of close to 0.3%.

3. Design of an Optical Wavelength FEL: Additional Design Considerations

Figs. 1 and 2 illustrate the basic FEL and accelerator configurations and Fig. 3 defines micropulses and macropulses. These figures are from reference 12 which is an excellent review of high power free electron laser technology. A table of recent FEL experiments is given in Table 2, from reference 21.

3.1 Long Micropulse Accelerators

The required FEL bandwidth, $\Delta\nu$, is limited to 0.1cm^{-1} which equals 3 GHz. This limit requires a micropulse length of 333 ps or longer in order to achieve the required transform limited bandwidth using the relation $(\Delta\nu)(\Delta t) \geq 1$. As an alternative, we may consider a somewhat shorter micropulse length, such as 200 ps. In that case, we would

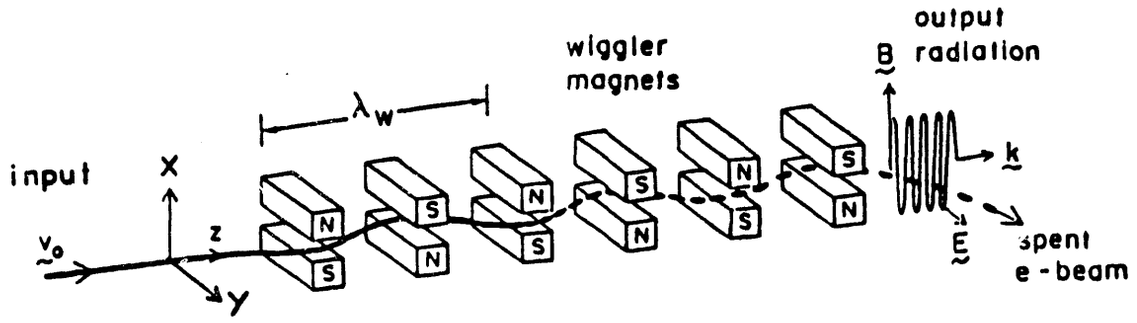

Fig. 1. Basic elements of a free-electron laser. Electrons are injected into an alternating periodic magnetic field produced by wiggler magnets as shown. The magnet array causes the electrons to oscillate in the y-z plane, parallel to the electric field, E, of the radiation. The transverse energy of the electrons is thereby coupled to, and amplifies, the radiation field. Although the radiation is shown at the wiggler output for simplicity, the interaction occurs over the entire length of the wiggler.

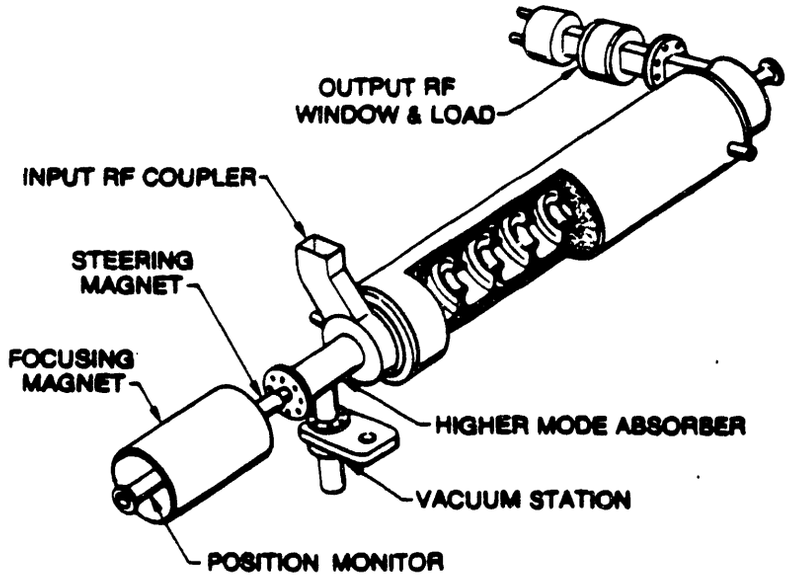

Fig. 2. Accelerator waveguide section, one of six, for the Boeing L-band linac. The design is typical of traveling-wave linac structures except for the contoured cells. The addition of high-order-mode probes between sections reduces the growth of deleterious transverse deflection modes.

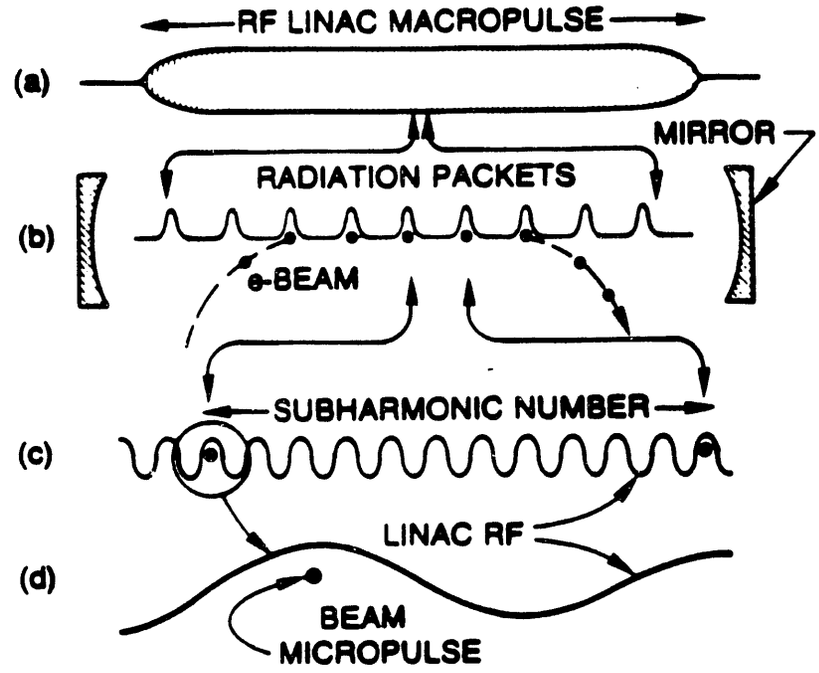

Fig. 3. Pulse timing sequence shows the time scale from macropulse to micropulse (values refer to the Boeing linac): (a) beam macropulse duration 200 μs; (b) schematic of FEL resonator mirrors, showing synchronization between radiation packets and beam micropulses. Effective mirror one-way transit time 221 ns; (c) beam micropulses occupy a maximum of 1 out of every 36 rf "buckets," for a spacing of 27.7 ns; (d) beam micropulse duration about 20 ps. Linac rf frequency: 1.3 GHz; macropulse repetition rate: 1 Hz.

Table 2 Free Electron Lasers

FEL	I (Amps)	γ	N	λ_0 (cm)	K	λ (μm)	w_0 (cm)	j	Comments
[3] Stanford '76	0.07	48	160	3.2	0.72	11	0.3	0.2	First A,RF,H
[4] Stanford '77	2.6	86	160	3.2	0.72	3.4	0.3	6	First O,RF,H
[69] Stanford '80	1.3	85	160	3.3	0.71	3.4	0.14	3.6	O,RF,H
[70] LANL '82	20	40	37	2.7	0.55	11	0.16	1.8	A,RF,L,$\delta=10\pi$
[71] MSNW/Boeing '83	3	38	91	2.5	0.44	11	0.16	2.8	A,L,$\delta=33\pi$
[72] TRW/EG&G '83	10	50	75	3.6	0.63	11	0.17	1.6	A,RF,L
[73] LANL '84	40	40	37	2.7	0.54	11	0.15	3.6	O,RF,L
[74] TRW/Stanford '84	2.5	130	153	3.6	0.97	1.6	0.1	3.4	O,RF,L,$\delta=4\pi$
[75] Orsay ACO '84	0.03	326	17	7.8	1.2	0.65	0.03	0.0005	A,SR,L,$D=100$
[76] Novosibirsk '84	7	686	22	6.9	2.7	0.62	0.03	0.06	A,SR,L,$D=280$
[77] Frascati ENEA '85	2.4	40	50	2.4	0.35	11	0.1	0.14	O,M,L
[78] Orsay ACO '85	0.2	432	17	7.8	2	0.63	0.03	0.004	O,SR,L,$D=100$
[79] UCSB '85	1.25	6.8	160	3.6	0.11	400	1	0.35	O,V,L
[80] INFN LELA '85	0.018	1224	20	12	3.5	0.51	0.04	0.00006	A,SR,L
[81] LLNL ELF '85	500	7.5	30	9.8	2.8	8700	1.5	9000	A,IL,L
[82] LANL '86	130	40	37	2.7	0.56	11	0.14	53	O,RF,L,$\delta=18\pi$
[83] Stanford Mark III '86	20	87	47	2.3	1.5	3.1	0.07	32	O,RF,L
[84] LLNL ELF '86	850	6.9	30	9.8	2.5	8700	1.5	14100	A,IL,L
[85] LLNL ELF Tapered '86	850	6.9	30	9.8	2.4	8700	1.5	14400	A,IL,L,$\delta=50\pi$
[86] LLNL ELF '87	1000	7.8	40	9.8	1.1	2000	1.5	7200	A,IL,L
[87] Boeing/Spectra '87	100	223	229	2.2	1.3	0.5	0.06	687	O,RF,L,$\delta=92\pi$
[88] Bell Labs	5	24	50	20	0.93	240	2	2	O,M,H
[89] BNL	22	588	39	6.5	2.3	0.6	0.07	0.25	A,SR,L
[90] United Kingdom	10	118	76	6.5	1.9	11	0.3	8.9	O,RF,L
[91] LANL XUV	100	400	750	1.6	0.79	0.08	1.6	414	O,RF,L
[92] Stanford XUV	270	1958	422	6.4	1.6	0.03	0.06	37	O,SR,L
[93] NBS XUV	2	363	130	2.8	1	0.23	0.04	0.6	O,M,L
[94] LBL/BNL XUV	200	1470	870	2.3	2.6	0.04	0.03	1360	SR,SRA,L
[95] Beijing PRC	15	40	50	3	1	11	0.1	5	O,RF,L

RF - RF Linac Accelerator, IL - Induction Linac Accelerator, M - Microtron Accelerator, SR - Electron Storage Ring, V - Van De Graaff Electrostatic Accelerator, H - Helical Undulator Polarization, L - Linear Undulator Polarization, δ=# - Tapered Undulator FEL, D=# - Klystron Undulator FEL, A - FEL Amplifier, O - FEL Oscillator
SRA - Super-Radiant Amplifier in a Long, Single-Pass Undulator

require that the power level must increase, by a factor of (333/200), in order to maintain 7 kW of average power in the 3 GHz bandwidth.

An RF accelerator produces bunches whose length is a small fraction of an RF cycle, typically less than 8°, in order to maintain a constant acceleration field strength over the part of the RF cycle utilized. The 8° limit arises because cos 8° equals 0.99 so that larger bunches in general can create more than 1% of energy spread. For a 433 MHz accelerator, an 8° bunch is 51 ps long; for 1.3 GHz, 17 ps long and for 2.856 GHz, 8 ps long. For these accelerators, the RF linac must be followed by a pulse stretcher to stretch the 8 to 51 ps bunch into the required 200-333 ps bunch length.

A low frequency accelerator, 50 to 100 MHz, would yield a 220-440 ps bunch length. However, such an accelerator would be much too large, would have a low acceleration gradient and would be very expensive. A 50 MHz accelerator, PHERMEX has been built at LANL[13,14], but it does not appear suitable for the present applications. High current RF linacs have been reviewed by Godlove and Sprangle, reference 12, and some examples are listed in Table 3.

3.2 Harmonic Accelerator

An alternate concept for accelerating micropulses that exceed the 8° limit was proposed in 1985 by Hess, Schwettman and Smith of Stanford. The concept requires cavities which have a small amount of third harmonic radiation supported in the same cavity as the fundamental. The sum of the two fields, at ω and 3ω could accelerate a 37° bunch with a 0.1% energy spread, as illustrated in Fig. 4. At present, high power klystrons are available for at least one pair of frequencies in the ratio of three to one, namely at 433 MHz and 1.3 GHz. An FEL using this set of frequencies is illustrated in Fig. 5. The micropulses in a 37° bunch from such an accelerator would be 237 ps long, adequate for the proposed FEL. The main drawback to this approach is that the concept has not yet been tested even at low power on a working RF linac. For this reason, it was not selected as the primary approach for the present design study.

3.3 Superconducting RF Linac Based FEL

A superconducting RF linac has several potential advantages for high average power applications including excellent stability. Such stability might be crucial to achieving the required narrow FEL bandwidth required in the present design. Further, superconducting

TABLE 3 HIGH-CURRENT RF LINACS

Linac (Purpose)	Boeing (FEL)	LANL (FEL)	Osaka (Multi)	ANL (Multi)	SLAC (Injector)	PHERMEX (Note 1)
Energy (MeV)	120	21	34	22	40	26
Freq. (MHz)	1300	1300	1300	1300	2856	50
I_p (A)	250	300	600	1000	600	400
Charge (nC)	4	4	10	25	8	1300
ε_n (mm-mrad)	50	120	57	480	150	260
$(A/m^2rad^2)\times10^{-9}$	20	4	28	0.9	5	1
dE/E (%)	1	1	1	1	1	10-30
T (μs)	200	120	Note 2	Note 2	1	0.2
Subharmonic	36	60	12	12	16	1
Rate (Hz)	1	10	720	1000	180	0.1
Reference	17	31	29	30	27	28

Symbols: I_p = peak micropulse current; T = macropulse duration;
ε_n = normalized edge emittance = $4\beta\gamma[\langle x^2\rangle\langle x'^2\rangle-\langle xx'\rangle^2]^{1/2}$;
B = brightness = $2I_p/(\pi\varepsilon_n)^2$ (Ref. 26).

Note 1: LANL facility used primarily for radiographic analysis.
Note 2: Produces a single micropulse, at the rate noted.

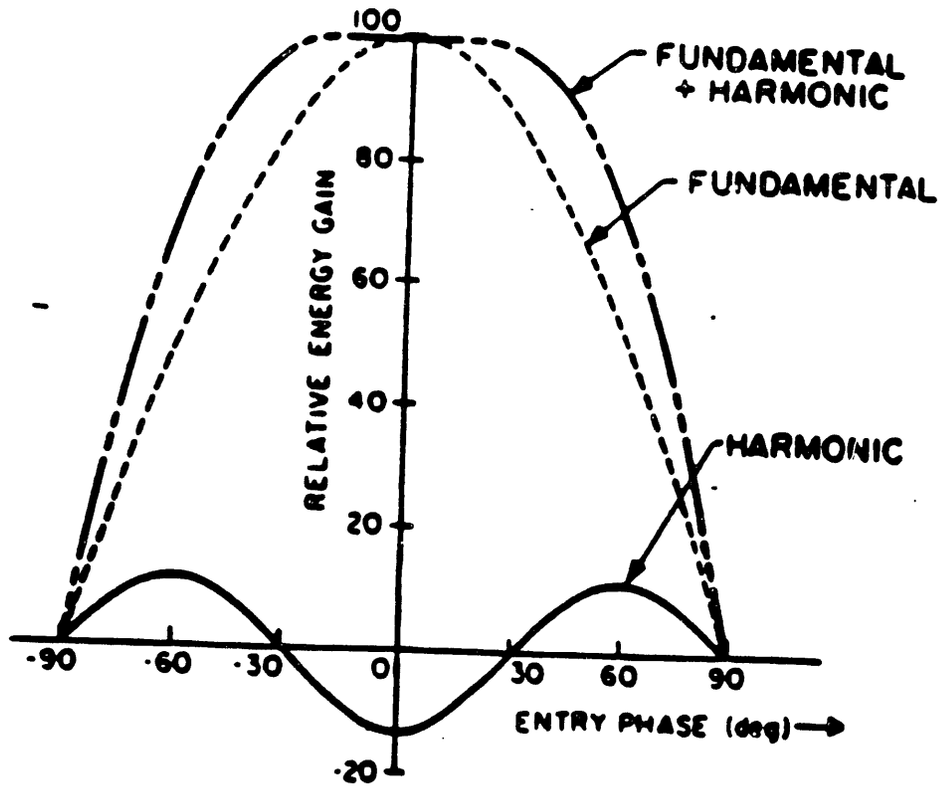

Fig. 4 Flat-topping the energy gain versus phase with a third harmonic cavity optimized for a 37° bunch: this yields a 0.1% energy spread. The fundamental and the summed fields are normalized to the same energy gain.

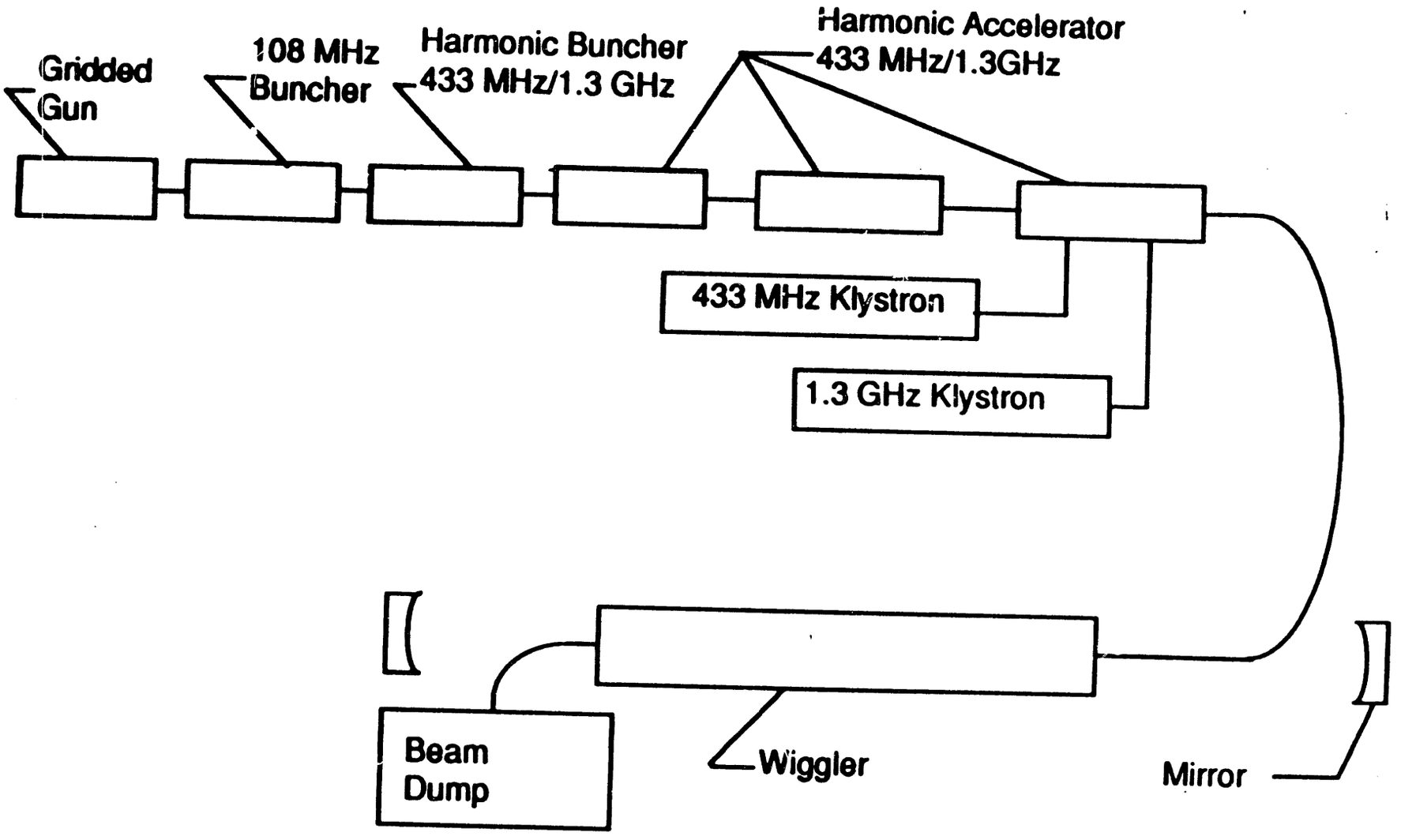

FREE ELECTRON LASER WITH HARMONIC ACCELERATOR

Figure 5

accelerators are under intensive development in support of new facilities such as CEBAF. A problem arises in applying a superconducting RF linac in the present design. The required pulse format is 100 μs macropulses at a 1 kHz repetition rate. A superconducting accelerator cavity typically has a cavity quality factor (Q) in excess of 10^8, with values greater than 10^9 routinely achieved, at frequencies below 1 GHz. A macropulse cannot be shorter than the cavity decay time which is given by (Q/ω). For a Q of 10^8 and a frequency ($\omega/2\pi$) of 500 MHz, the cavity decay time is 32 ms, or 320 times longer than the required 100 μs macropulse length. The use of a superconducting RF accelerator is thus ruled out and only a conventional accelerator with copper cavities will be further considered.

3.4 Storage Ring FEL

The storage ring has been very successfully applied to a visible wavelength FEL both in France[16,17], the Aco and Super Aco devices at Orsay, and in the Soviet Union on the VEPP 3-device at Novosibirsk[18,19]. The storage ring is attractive for several reasons. First, visible and even ultraviolet wavelength emission have been obtained from storage ring FELs. Second, the micropulse length in a storage ring tends to be relatively long, as long as 330 ps in the VEPP-3 ring. Third, the electron beam quality in a storage ring is very high with demonstrated energy spread as low as $\Delta\gamma/\gamma$ of 10^{-3}. Fourth, compact, high power storage rings are under intensive development for x-ray lithography resulting in reduced system cost. In addition to these general considerations, storage ring FELs have already demonstrated extremely narrow bandwidth emission at visible wavelengths. A laser bandwidth for the VEPP-3 storage ring of $\Delta\lambda/\lambda$ of 1^{-4} was reported at the Eleventh FEL conference in 1989.

In these respects, the storage ring FEL might seem ideal for the present application. However, the stable passage of the electron beam through the ring and wiggler for many transits limits the output power of the FEL according to the theorem of Renieri. The FEL output power limit is basically given by the product of the synchrotron power emitted by the electron beam in the ring times the energy acceptance ($\Delta\gamma/\gamma$) of the wiggler. The time average output power would then be limited to Watts rather than kilowatts. The Renieri limit is only a simple model of the storage ring FEL and the power can be increased by use of an isochronous storage ring[20]. At present, this concept is unverified and will therefore not be selected for further analysis at this time. The physics results, indicating excellent emission bandwidth from a stable, 300 ps micropulse storage ring FEL, are encouraging for the FEL system proposed here.

3.5 1.3 GHz Accelerator

Although a number of approaches are potentially feasible for the proposed optical wavelength FEL, a conventional RF linac based FEL seems the most attractive. The conventional RF linac has widespread application at high average power[12]. The Boeing FEL system uses a conventional 1.3 GHz accelerator with a copper accelerator structure[25]. That FEL has operated at wavelengths near 60 nm using an electron beam with an energy as high as 120 MeV. A system based on the Boeing design but scaled up to high average power represents a viable design option for a 7 kW power level, visible wavelength FEL. The present design requirement differs from the Boeing system primarily in the use of long micropulses, 330 ps vs. 8-20 ps.

A number of high power, RF acclerators have been constructed at frequencies of 0.433, 1.30 and 2.856 GHz. Accelerators are feasible at other frequencies, but the klystron and structure technology are less developed at other frequencies. The use of a frequency of 1.3 GHz assures that klystrons of the proper peak power, estimated to be about 5-10 MW, and average power, estimated to be about 100 kW, are available. The use of a 1.3 GHz accelerator has several additional advantages over the 0.433 GHz accelerator. The size, weight and cost of the accelerator vary roughly as the wavelength squared. This means that a 1.3 GHz accelerator has a significant advantage. On the other hand, very high average power klystrons, exceeding 100 kW, are not presently available at 2.856 GHz. This fixes the accelerator frequency at 1.3 GHz for the present device. We would like to acknowledge the assistance of Dr. J. Haimson of Haimson Research in Palo Alto and Mr. Tremeau of Thomson TTE in Paris regarding 1.3 GHz accelerator and klystron technology.

The use of a conventional, 1.3 GHz accelerator results in an electron beam with 20 ps micropulses. The present design will require a pulse stretcher after the accelerator to increase the micropulse length from 20 to over 200 ps. A detailed analysis of the effect of pulse stretching on the electron beam quality is important but is beyond the scope of this study. A detailed design of a similar pulse stretcher for a 1.3 GHz accelerator has been considered at Los Alamos (D. Prono and L. Thode, LANL, private communication).

3.6 FEL Bandwidth

The required FEL bandwidth is:

$$\frac{\Delta\nu}{\nu} = \frac{\Delta\lambda}{\lambda} \approx 5 \times 10^{-6}$$

An FEL has a small signal, "homogeneous" bandwidth, for an untapered wiggler of N periods, given by

$$\frac{\Delta\nu_{HOM}}{\nu} \approx \frac{1}{2N} = 2 \times 10^{-3}$$

where a typical value of N of 200 periods has been assumed. This indicates that the required FEL bandwidth for the present design is 500 times smaller than the FEL gain bandwidth. We can expect some line narrowing to occur in any laser medium having expontial gain. This line narrowing occurs during the onset of laser oscillation, in the small signal gain regime. The resultant line narrowing for the FEL has been analyzed by Colson[21] and is given by:

$$\frac{\Delta\nu}{\Delta\nu_{HOM}} = \frac{0.7}{\sqrt{\gamma L}}$$

where γ is the gain coefficient per unit length and L is the total gain length (cavity length times the number of round trips). For a typical value of $\gamma L \approx 30$, the line is narrowed by a factor of about 8 leading to a bandwidth of:

$$\frac{\Delta\nu}{\nu} \approx 3 \times 10^{-4}$$

This bandwidth is still 60 times larger than the required bandwidth. Furthermore, as the laser saturates, the bandwidth will increase. The sidband instability in an FEL can cause a dramatic increase in the frequency bandwidth with values of $\Delta\nu/\nu$ exceeding 1% observed in several FEL experiments.

In order to achieve the required bandwidth, it is therefore necessary to introduce an optical line narrowing element into the FEL cavity. One approach that has been suggested for visible wavelength FELs is the grating rhomb[22,23]. Simulations show that the grating rhomb can eliminate sidebands and yield a narrow, efficient laser output pulse. It would be useful to explore the possibility of achieving a bandwidth as small as 0.1cm^{-1}, as required in the present design, using grating rhombs in an FEL oscillator. This analysis was begun at the end of the first year of this program and is proposed for additional study in the second year.

3.7 Amplifier vs. Oscillator Designs

The use of an FEL oscillator results in the simplest design for a 7 kW, visible wavelength FEL. However, it is not clear that the bandwidth requirement can be met in practice

with an FEL oscillator, as discussed in the previous section. It is possible that FEL amplifier designs, injecting a low power, narrow bandwidth driver signal from an oscillator, would allow the bandwidth requirement to be met.

The availability of high power glass lasers to serve as the driver for an FEL amplifier may allow an attractive system design. Glass lasers putting out up to 0.1 J in 100 μs macropulses at high repetition rate could be used as drivers[24]. The required saturated gain in the FEL would then be about 70. This idea was investigated theoretically, as described below in Section 4. An alternate concept would be the use of harmonic generation in combination with an FEL system. An FEL could be operated at a wavelength of 1.0 to 1.2 μm and its output converted to 0.5 to 0.6 μm by second harmonic generation in a nonlinear crystal. The advantage of this approach is that the FEL uses a lower voltage beam, by a factor of 0.707, for 1.0 μm emission than for 0.5 μm. This may save up to 30% in cost for the FEL electron accelerator. There is an additional benefit in that the FEL gain and efficiency are higher at the longer wavelength. These ideas were explored on a preliminary basis in this program and they merit further consideration.

4. Nonlinear Model of FEL: Gain and Efficiency Calculations

In this section, we describe the system of equations governing the motion of the individual electrons and the self-consistent evolution of the electromagnetic fields in a FEL.

4.1 Single Particle Motion

We consider a circularly polarized magnetostatic wiggler characterized by the vector potential

$$\mathbf{A}_w = -\frac{mc^2}{e} a_w[\hat{\mathbf{e}}_x \cos(k_w z) - \hat{\mathbf{e}}_y \sin(k_w z)], \tag{1}$$

where $a_w = a_w(x, y, x)$ and $k_w = 2\pi/\lambda_w$ are the wiggler field amplitude and wave number. The induced electromagnetic field is circularly polarized with vector potential of the form

$$\mathbf{A}_s = \frac{mc^2}{e} a_s[\hat{\mathbf{e}}_x \cos(k_s z - \omega_s t + \phi_s) + \hat{\mathbf{e}}_y \sin(k_s z - \omega_s t + \phi_s)], \tag{2}$$

where $a_s = a_s(x, y, z, t)$, $\phi_s(x, y, z, t)$, k_s and ω_s are the transverse electromagnetic field's amplitude, phase, wave number and frequency, respectively. The complex amplitude $a_s \exp(i\phi_s)$ is assumed to be a slowly varying function of the longitudinal coordinate z and the time t (eikonal approximation):

$$\left|\frac{\partial}{\partial z} \ln a_s e^{i\phi_s}\right| \ll k_s, \quad \left|\frac{\partial}{\partial t} \ln a_s e^{i\phi_s}\right| \ll \omega_s. \tag{3}$$

When the current is sufficiently low, which is the case for the parameters chosen in the present study (Table 4), the electrostatic interaction can be neglected (Compton regime approximation), and the equations of motion of a single electron are completed determined, given the transverse potential defined in Eqs. (1) and (2). The Hamiltonian describing the motion of the particle through the wiggler can be expressed in the following dimensionless form[26]:

$$h(x, p_x, y, p_y, ct, -\gamma|z) = -\sqrt{\gamma^2 - 1 - p_x^2 - p_y^2 - a_x^2 - a_y^2 + 2(p_x a_x + p_y a_y)}. \tag{4}$$

Here, $a_x = (A_{wx} + A_{sx})(e/mc^2)$ and $a_y = (A_{wy} + A_{sy})(e/mc^2)$ are the transverse components of the normalized vector potential of the combined wiggler and electromagnetic fields. Furthermore, the canonical momenta (normalized to mc) p_x, p_y and

the negative of the relativistic Lorentz factor γ, play the role of the momenta conjugate to the coordinates x, y and ct, respectively, with the coordinate z being the independent variable. The Hamiltonian equations are then

$$\frac{d\mathbf{p}_\perp}{dz} = -\frac{\partial h}{\partial \mathbf{r}_\perp}, \quad \frac{d\mathbf{r}_\perp}{dz} = \frac{\partial h}{\partial \mathbf{p}_\perp}, \quad \frac{d(-\gamma)}{dz} = -\frac{\partial h}{\partial (ct)}, \quad \frac{d(ct)}{dz} = \frac{\partial h}{\partial (-\gamma)}, \tag{5}$$

where the '$\perp$' symbol designates the x, y transverse components. By taking an appropriate average of the Hamiltonian h over the wiggler period λ_w, the last term in parenthesis in Eq. (4) can be eliminated. Retaining only the first term in the expansion in $1/\gamma$ yields

$$h(x, p_x, y, p_y, ct, -\gamma | z) = -\gamma + \frac{1 + |\mathbf{p}_\perp|^2 + |\mathbf{a}_\perp|^2}{2\gamma}. \tag{6}$$

From the expressions for the vector potentials given in Eqs. (1) and (2), it follows that

$$|\mathbf{a}_\perp|^2 \equiv a_x^2 + a_y^2 = a_w^2 + a_s^2 - 2a_w a_s \cos(\theta + \phi_s). \tag{7}$$

Here, we have introduced the particle "phase" θ, defined by

$$\theta(z) = (k_w + k_s)z - \omega_s t(z). \tag{8}$$

From Eq. (5), the averaged motion of an electron in the combined wiggler and electromagnetic fields is determined by the following first order equations:

$$\frac{d\mathbf{p}_\perp}{dz} = -\frac{1}{2\gamma}\frac{\partial |\mathbf{a}_\perp|^2}{\partial \mathbf{r}_\perp}, \tag{9}$$

$$\frac{d\mathbf{r}_\perp}{dz} = \frac{\mathbf{p}_\perp}{\gamma}, \tag{10}$$

$$\frac{d\gamma}{dz} = -\frac{\omega_s}{\gamma c} a_w a_s \sin(\theta + \phi_s), \tag{11}$$

$$\frac{d\theta}{dz} = k_w - \frac{\omega_s}{c}\frac{1 + |\mathbf{p}_\perp|^2 + a_w^2 + a_s^2 - 2a_w a_s \cos(\theta + \phi_s)}{2\gamma^2}, \tag{12}$$

$$\frac{d(ct)}{dz} = 1 + \frac{1 + |\mathbf{p}_\perp|^2 + a_w^2 + a_s^2 - 2a_w a_s \cos(\theta + \phi_s)}{2\gamma^2}. \tag{13}$$

4.2 Field Equations

The evolution of the transverse electromagnetic field can be determined from the Maxwell's equations

$$\left(\nabla^2 - \frac{1}{c^2}\frac{\partial^2}{\partial t^2}\right)\mathbf{A} = -\frac{4}{c}\mathbf{J}. \tag{14}$$

The transverse current can be constructed by adding the contribution from the electrons, i.e.,

$$J_x + iJ_y = -e\sum_j^N \frac{\beta_{xj} + i\beta_{yj}}{\beta_{zj}}\delta^2(\mathbf{r}_\perp - \mathbf{r}_{\perp j})\delta(t - t_j), \tag{15}$$

where $\mathbf{r}_{\perp j} = \mathbf{r}_{\perp j}(z)$ and $t_j = t_j(z)$ denote the trajectory of the jth particle. The transverse velocities β_{xj} and β_{yj} can be related explicitly to the transverse canonical momenta p_{xj}, p_{yj} by

$$\gamma_j\beta_{xj} + i\gamma_j\beta_{yj} = -a_w e^{-ik_w z} + a_s e^{i(k_s z - \omega_s t + \phi_s)} + p_{xj} + ip_{yj}. \tag{16}$$

Note that the expression for the current in Eq. (15) is strongly fluctuating due to the singular behavior of the delta function. Therefore, to determine the slow evolution of the complex amplitude $a_s e^{i\phi_s}$, we average Eq. (14) over the fast time scale $T = \omega_s^{-1}$. Moreover, making use of the eikonal approximation in Eq. (3) to neglect the second-derivative terms $(\partial^2/\partial t^2)$ and $\partial^2/\partial z^2$, Eq. (14) reduces to

$$\left[\nabla_\perp^2 + 2ik_s\left(\frac{\partial}{\partial z} + \frac{1}{v_g}\frac{\partial}{\partial t}\right)\right]a_s e^{i\phi_s} = -\frac{4\pi e^2}{mc^3}\left[\frac{1}{T}\left\langle\frac{a_w e^{-i\theta}}{\gamma\beta_z}\right\rangle - \frac{1}{T}\left\langle\frac{a_s e^{i\phi_s}}{\gamma\beta_z}\right\rangle\right]. \tag{17}$$

Here, assuming there are N_T electrons in one period $(T = 2\pi/\omega_s)$, the time average $< (\cdots) > /T$ is defined by

$$\langle(\cdots)\rangle = \frac{1}{T}\sum_j^{N_T}\delta^2(\mathbf{r}_\perp - \mathbf{r}_{\perp j})(\cdots). \tag{18}$$

Although the averaged current on the right hand side of Eq. (17) still fluctuates strongly in the transverse directions, it will be smoothed out in numerical simulations by introducing some finite-size grids in the transverse directions.

4.3 Numerical Simulations

In studying the optimization of the FEL performance under conditions of realistic electron beam qualities, use is made of an FEL code TDA[27] to carry out computer simulations of the FEL interaction.

4.4 Description of the FEL Code TDA

The FEL code TDA simulates the FEL interaction by solving the coupled electron dynamics equations (9) - (13) and the field equation (17) self-consistently. The code allows for the treatment of the fully three-dimensional electron dynamics, thus taking into account the transverse betatron motion as well as the longitudinal bunching of the electrons. The paraxial wave equation that governs the growth and the diffraction of the self-consistent radiation field (assumed to be axisymmetric), is discretized in the radial direction by the finite difference method. The benchmark study indicates that the single-pass gain, as well as the optical guiding phenomena can be well described by the code with a reasonable number of simulation particles ($N \sim 1000$) and a radial mesh number not exceeding 64. The code may also take into account the space charge effects and the waveguide boundary condition. However, for the system parameters chosen in the present study (Table 4), the current is sufficiently low such that the space charge effects are negligible (Compton regime approximation). Moreover, in the present design the radiation is propagating in free space. Listed in Table 5 are the important features of the TDA code. Although it is an amplifier code, the oscillator configuration is simulated by converting the single pass code to its multi-pass version.

The code also includes field tapering[26], which is an efficiency enhancement scheme. For a fixed-period wiggler, the radiation field reaches its maximum value when the electrons are trapped in the longitudinal potential wells formed by the beating of the wiggler field and the radiation field. The longitudinal potential is moving with velocity $v_{\rm ph} = \omega_s/(k_s + k_w)$. If this phase velocity is appropriately reduced as a function of axial distance by decreasing the period of the wiggler $\lambda_w = 2\pi/k_w$, the kinetic energy of the electrons can be further reduced and converted into radiation energy. Efficiency enhancement can also be achieved by decreasing the wiggler field strength to speed up the axial velocity of the electrons.

4.5 Results of the Numerical Simulations

Numerical simulations have been carried out for the system parameters listed in Table 4. Except for those cases where specific values of the peak current are

TABLE 4

MIT Optical FEL Simulation Parameters

Electron Beam Energy:	U = 120 MeV
(For $\lambda = 0.5\mu$m)	$\gamma = 236$
Energy Spread, full width	$\Delta\gamma/\gamma$ 0.1 – 0.3%
Peak Electron Beam Current:	I = 25 – 50 A
Peak Electron Beam Power:	3 – 6 GW
Micropulse Length:	330 ps
Micropulse separation:	80 ns
Macropulse length:	100 μs
Macropulse repetition rate:	1 kHz
Electron beam emittance:	ϵ_N =250 mm mrad
Electron beam radius:	r_{eo} = 0.40 mm
Macropulse average electron current:	100 – 200 mA
Macropulse average electron beam power:	12 – 24 MW
Wiggler period:	λ_w = 2.0 cm
Wiggler length:	Total length, 4m (200 periods)
Magnetic wiggler field:	$B_0 = 1.0$T $\quad a_w = 1.33$
Magnetic gap:	4 mm (approx.)
Betatron wavenumber:	$k_\beta = a_w k_w/\sqrt{2}\gamma = 1.22 \times 10^{-2}$cm^{-1}
Betatron period:	$L_\beta = 2\pi/k_\beta = 5.1$m
Optical beam waist:;	w_0 =0.4 mm
Rayleigh range:	$Z_R = \pi w_0^2/\gamma = 1$m

TABLE 5

TDA Axisymmetric FEL Simulation

- Fully Three Dimensional Code
- Single Pass FEL Amplifier Simulation
- Includes Space Charge Effects, Emittance and Beam Focussing by Transverse Wiggler Field
- Takes into Account Betatron Motion and Longitudinal Bunching, and Predicts Synchrotron Oscillations
- Includes Wave Diffraction, Non-uniform (tapered) wiggler profile
- Includes Waveguide Modes
- Includes Effects of Random Wiggler Field Errors, both Uncorrelated and Correlated

indicated, the peak electron beam current is 50A, which corresponds to an average electron current of 200mA and a macropulse average electron beam power of 24MW.

Shown in Fig. 6 is the FEL gain as a function of the axial distance for an input power (micropulse peak power) of 70MW. The FEL gain reaches a maximum value of 1.42 at $z \simeq 1.5$m and starts oscillating, as the radiation travels further down in the interaction region, due to the trapping of electrons in the longitudinal potentials. Figure 7 illustrates the evolution of the optical beam radius. The optical beam is focused to a minimum radius of 0.2mm (half of the waist) at $z = 1.1$m, and then expands due to diffraction.

The results of the FEL gain as a function of input power are shown in Fig.8. The results are given for $\delta\gamma/\gamma$ of 0.3% and a beam emittance ϵ_n of 25π mm-mrad. A few results for smaller energy spread and emittance are also listed. The results are shown for a linear taper of 0%, 1% and 2% in the wiggler field. The predicted efficiency per pass for the conditions of Fig. 8 are shown in Fig. 9. The potential of achieving 2% efficiency by wiggler field tapering is illustrated in Fig. 10, in which efficiency is plotted for different choices of current and energy spread $\delta\gamma/\gamma$ with an input power of 1000MW.

Using the results of Fig. 8 and an output coupling of 24% per pass, the growth of power in an FEL oscillator is shown in Fig. 11. The power is allowed to build up in the oscillator from a noise level of about 1W. Buildup occurs in about 8 round trips which is 640ns in the present design. This is very short compared to the FEL macropulse time of 100μs. For this example, the peak output power is 31.7MW and the time average output power is 12.7kW.

An alternate concept is an FEL amplifier driven by a glass laser oscillator. In Fig. 12, the average FEL output power is plotted as a function of the average input power for an untapered FEL amplifier. It is found that the input power required to reach the proposed 7kW output power is about 800W. Various strategies can be used to obtain higher gain; therefore less input power is required to achieve the same output power. Two examples of such strategies are wiggler field tapering and more wiggler periods. Figure 13 shows the gain versus length in the wiggler for an FEL amplifier. With a 14m wiggler, 0.2% wiggler field tapering and a time average input power of 400MW (or 1MW peak power), the time average output is 10kW and the

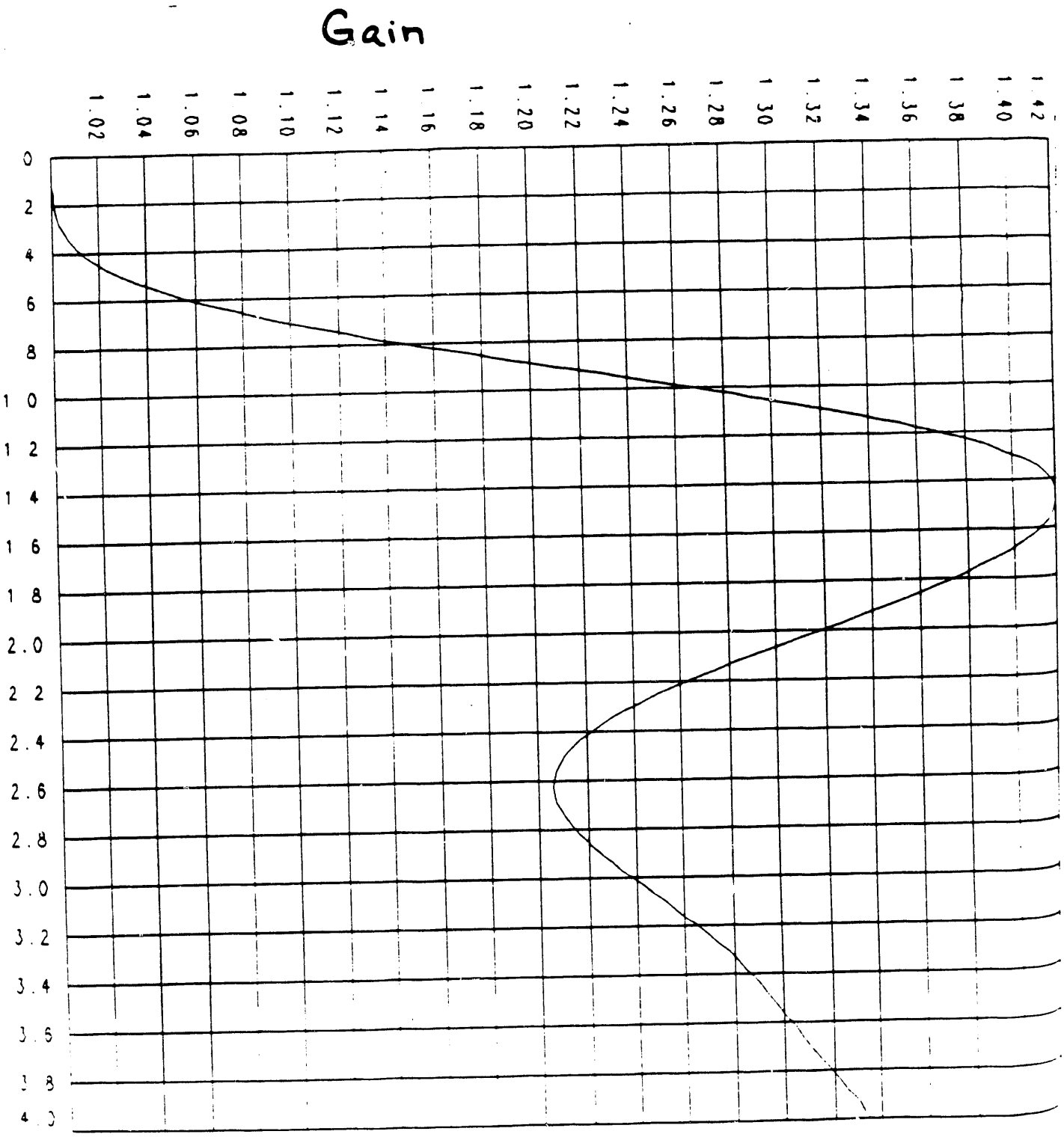
Gain
1.02
1.04
1.06
1.08
1.10
1.12
1.14
1.16
1.18
1.20
1.22
1.24
1.26
1.28
1.30
1.32
1.34
1.36
1.38
1.40
1.42
0
2
4
6
8
10
12
14
16
18
2.0
2.2
2.4
2.6
2.8
3.0
3.2
3.4
3.6
3.8
4.0
Z (m)
HISTORY OF POWER GAIN
P_{in} = 70 MW

Figure 6

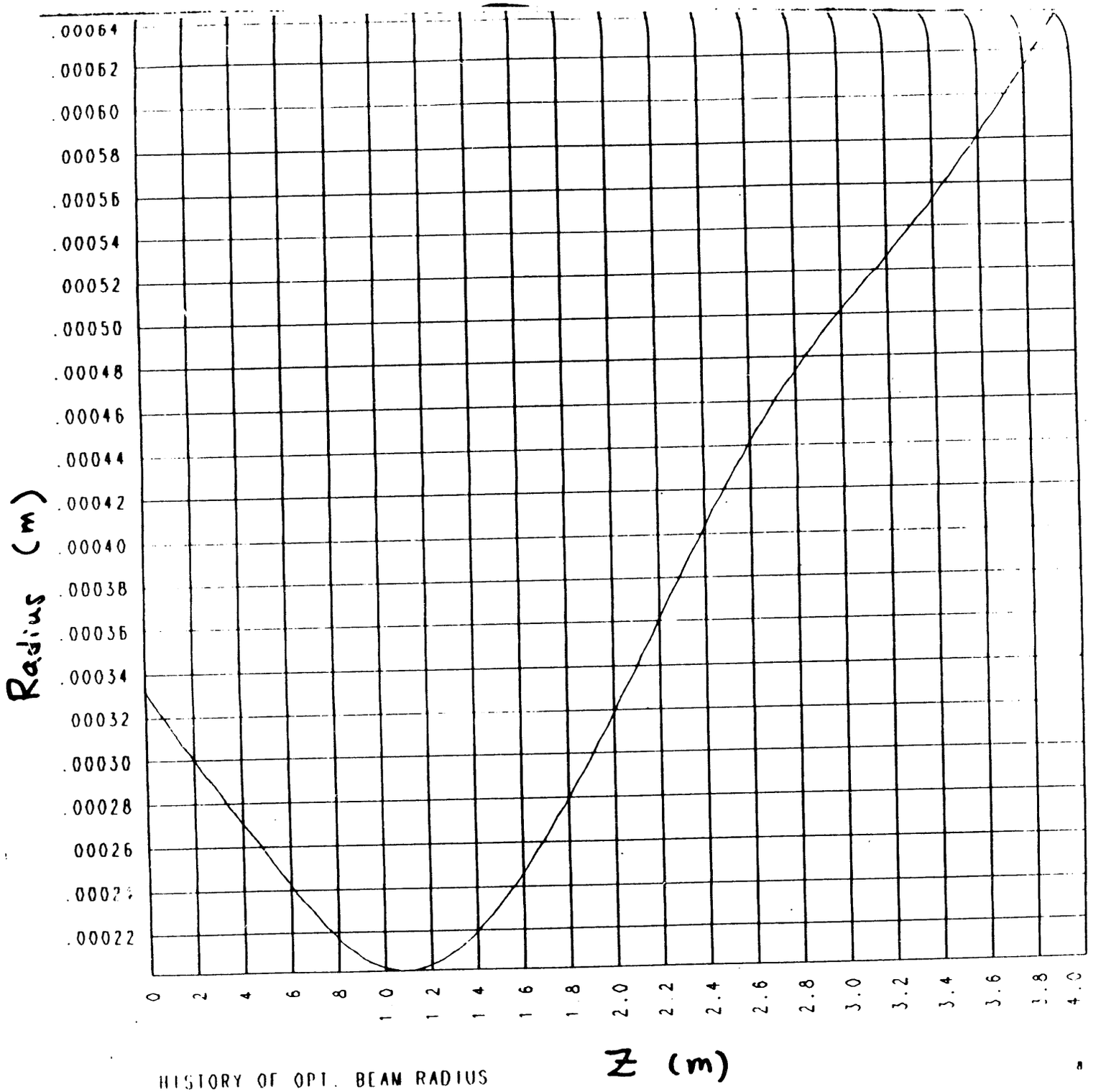
P_{in}= 70MW
Radius (m)
.00064
.00062
.00060
00058
.00056
.00054
00052
.00050
.00048
.00046
.00044
.00042
.00040
.00038
.00036
.00034
00032
.00030
.00028
00026
.00022
0
2
4
6
8
1 0
1 2
1 4
1 6
1 8
2.0
2.2
2.4
2.6
2.8
3.0
3.2
3.4
3.6
4.0
Z (m)
HISTORY OF OPT. BEAM RADIUS

Figure 7

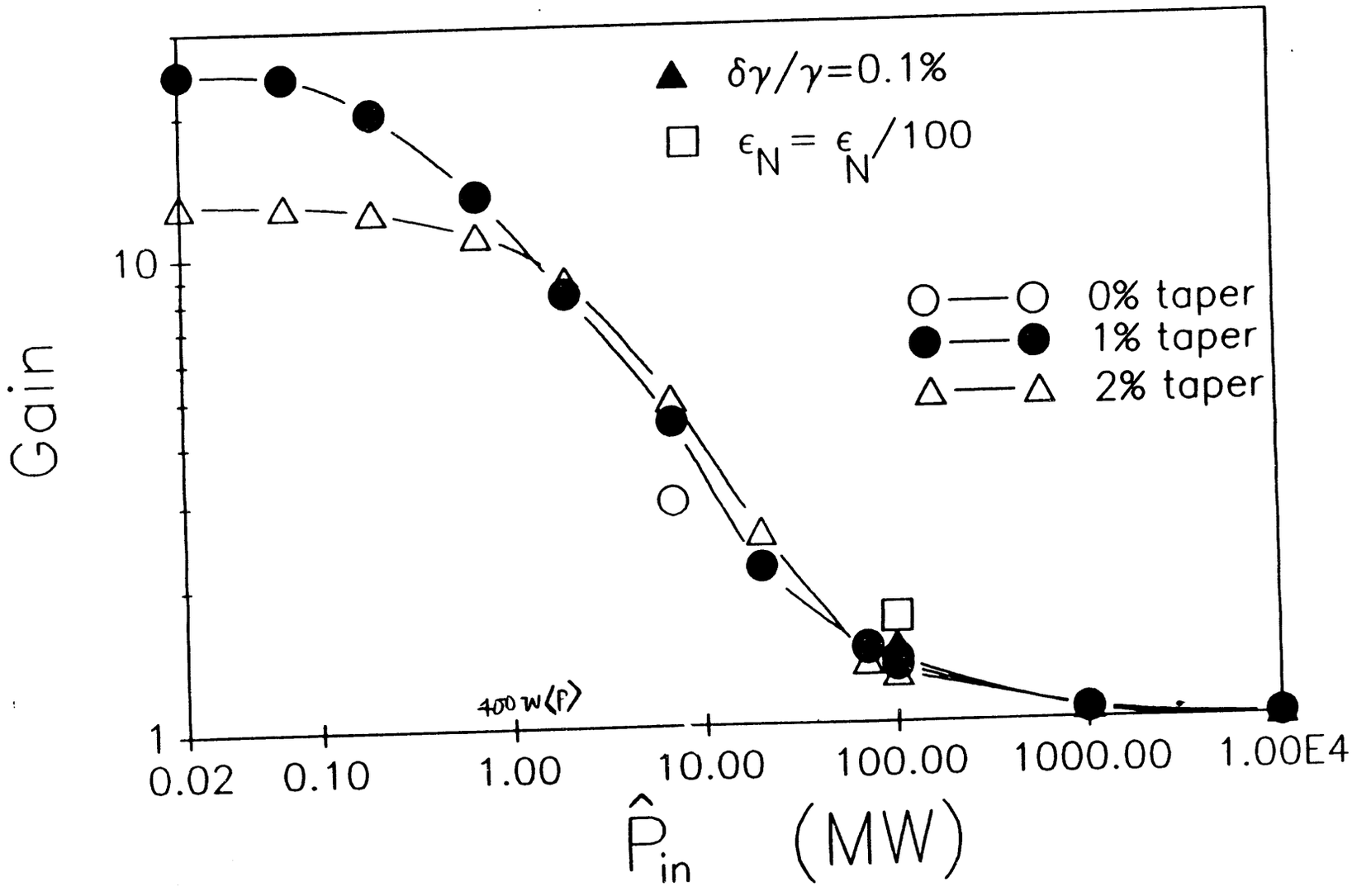
▲ δγ/γ=0.1%
□ $\epsilon_N = \epsilon_N/100$
○—○ 0% taper
●—● 1% taper
△—△ 2% taper
Gain
10
1
400 w⟨P⟩
0.02
0.10
1.00
10.00
100.00
1000.00
1.00E4
$\hat{P}_{in}$ (MW)

Figure 8

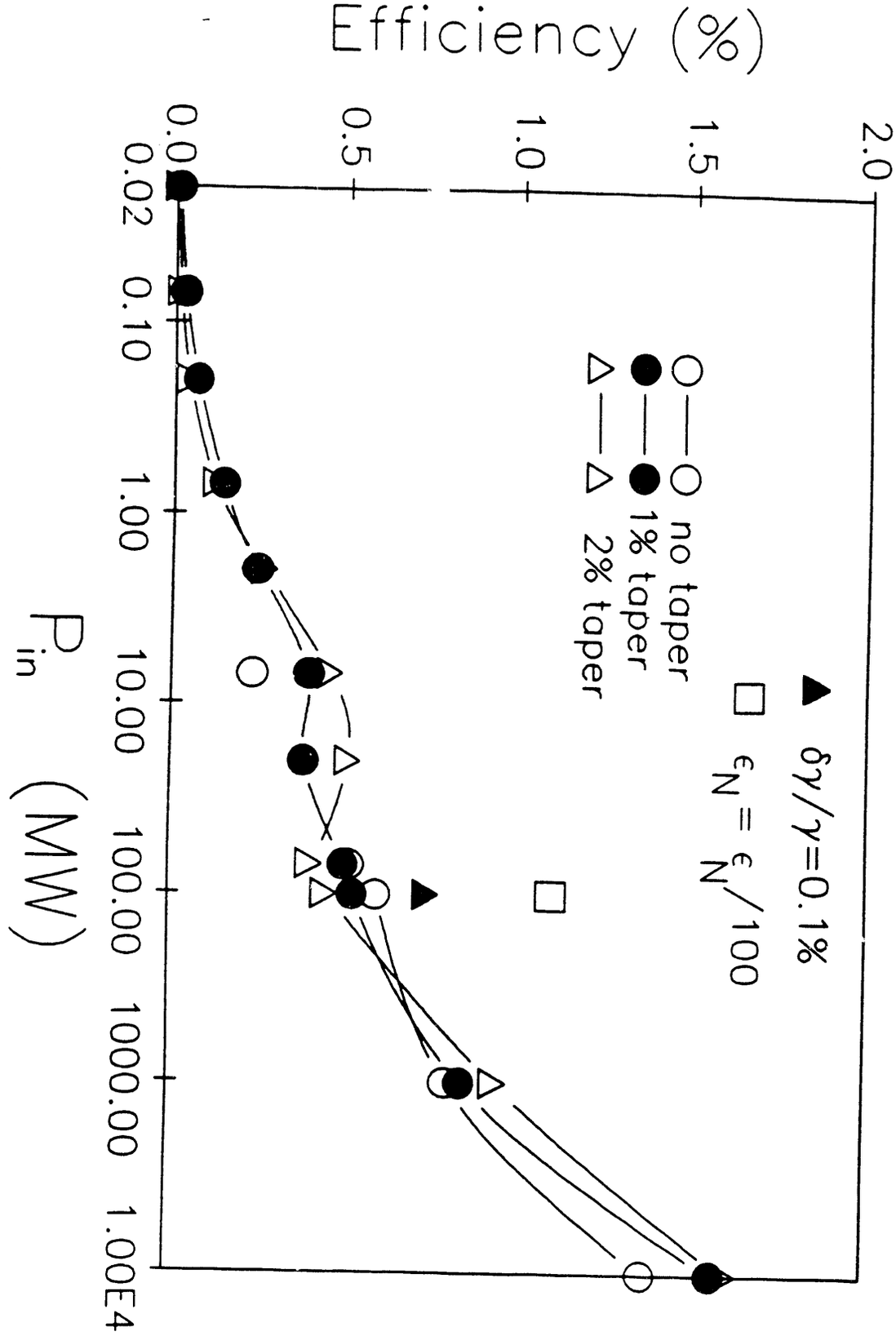
Efficiency (%)
0.0
0.5
1.0
1.5
2.0
0.02
0.10
1.00
10.00
100.00
1000.00
1.00E4
P_{in} (MW)
no taper
1% taper
2% taper
$\delta\gamma/\gamma$=0.1%
$\epsilon_N = \epsilon_N/100$

Figure 9

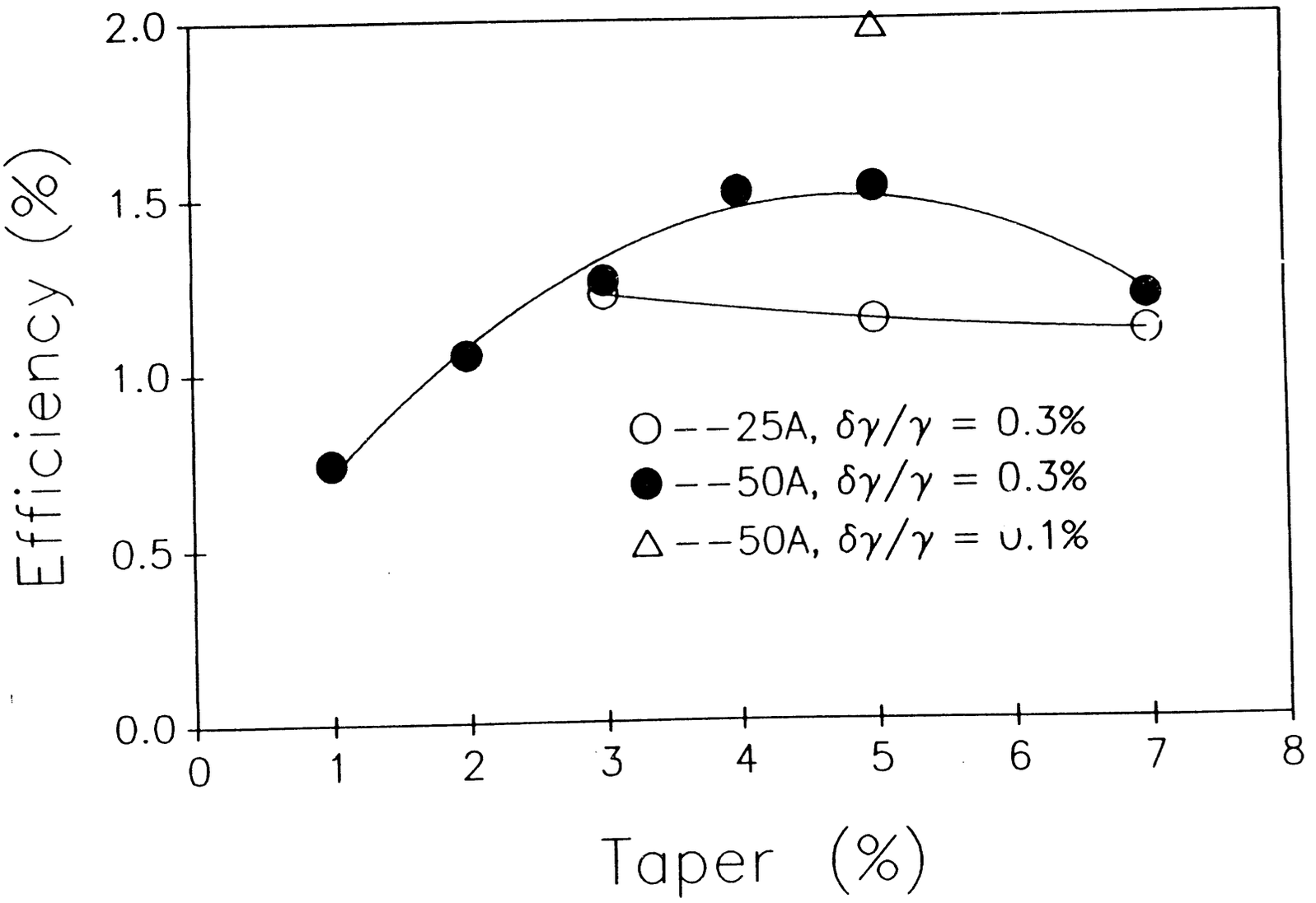
Efficiency (%)
2.0
1.5
1.0
0.5
0.0
0
1
2
3
4
5
6
7
8
Taper (%)
○ --25A, δγ/γ = 0.3%
● --50A, δγ/γ = 0.3%
△ --50A, δγ/γ = υ.1%

Figure 10

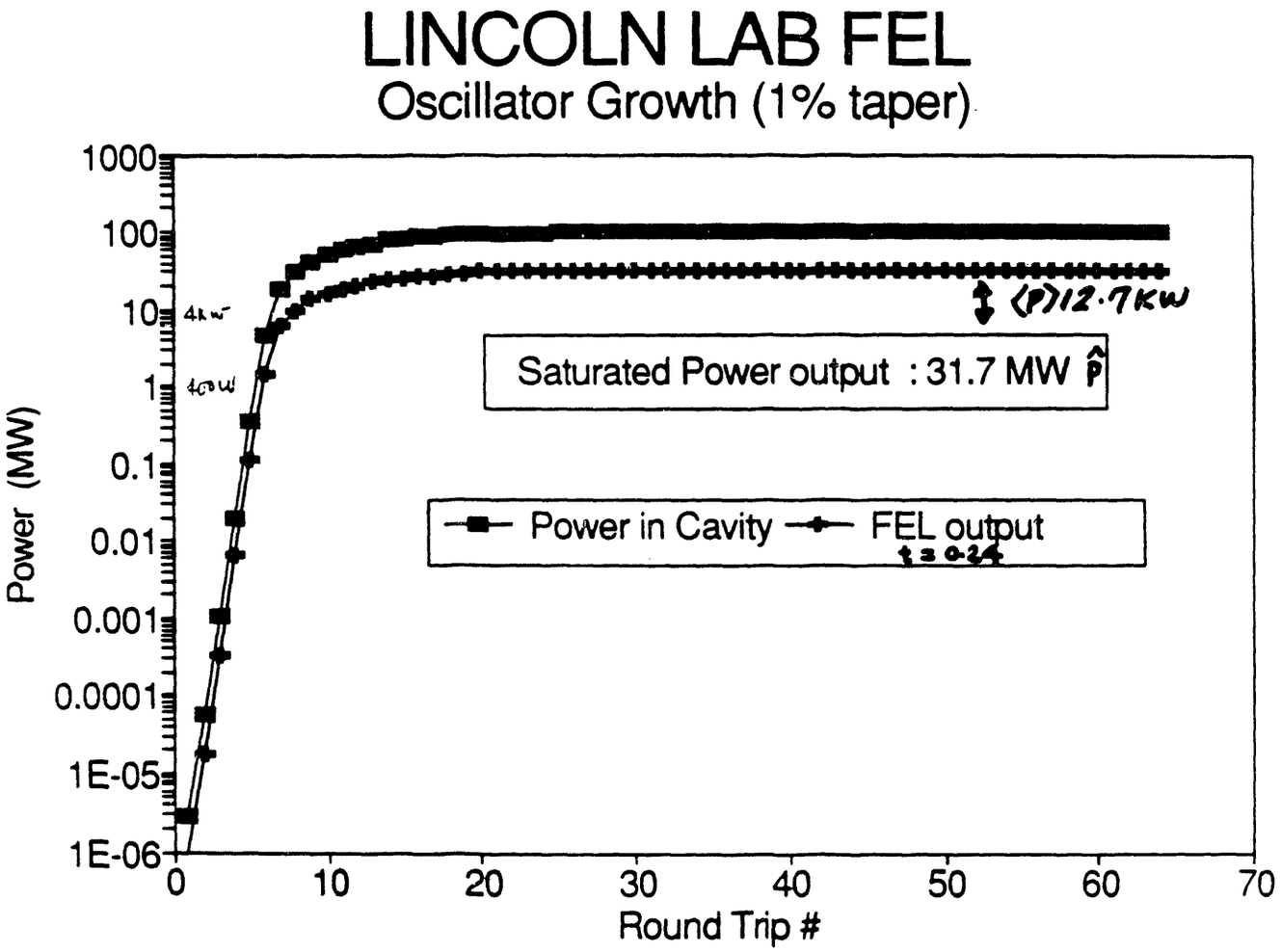

$L_{cavity} = 8m$ $\quad \tau_m / \frac{2L_{cavity}}{c} = 1875$ (pulses/macropulse)

Figure 11

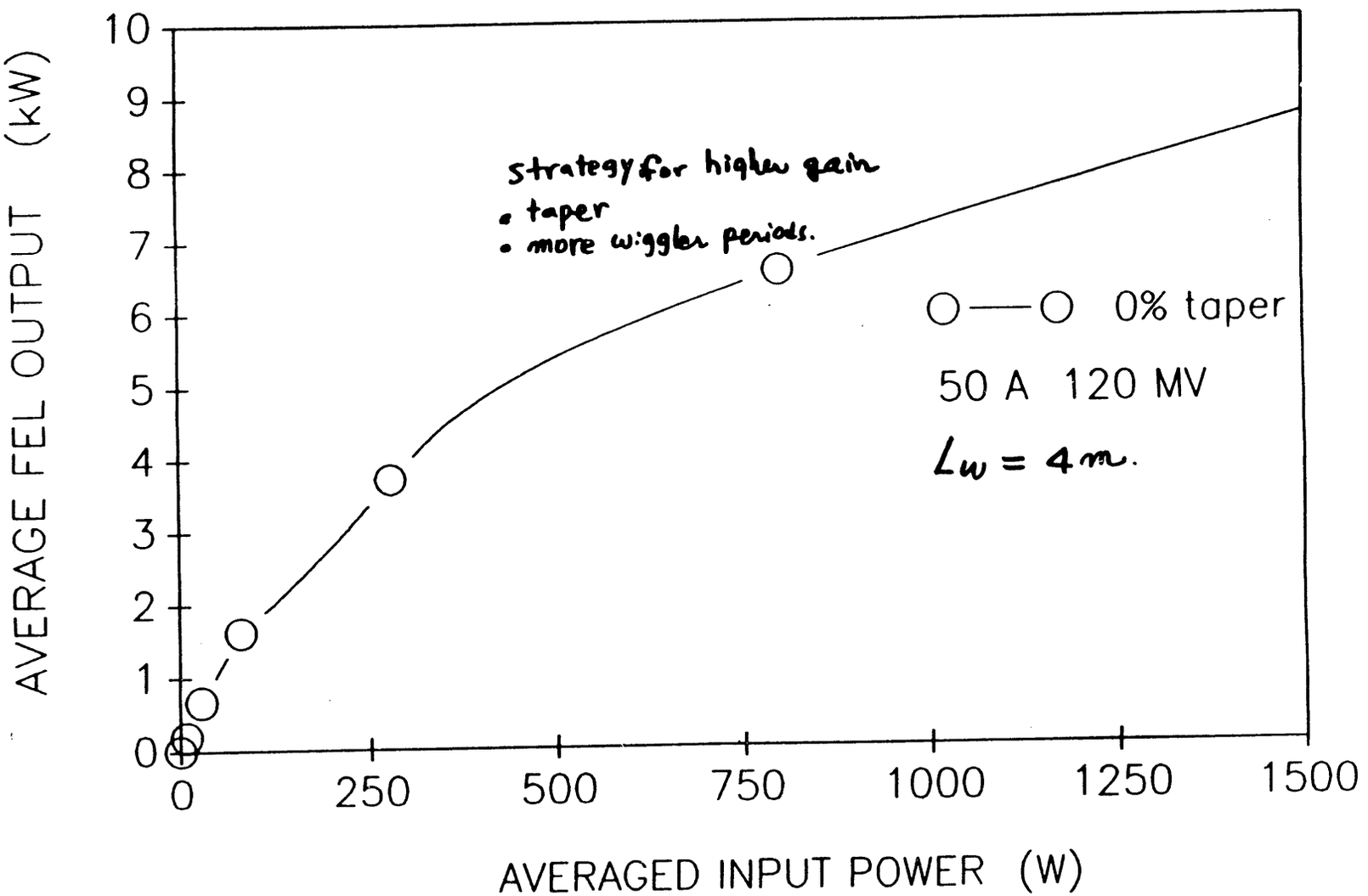
AVERAGE FEL OUTPUT (kW)
10
9
8
7
6
5
4
3
2
1
0
0
250
500
750
1000
1250
1500
AVERAGED INPUT POWER (W)
strategy for higher gain
• taper
• more wiggler periods.
O—O 0% taper
50 A 120 MV
Lw = 4 m.

Figure 12

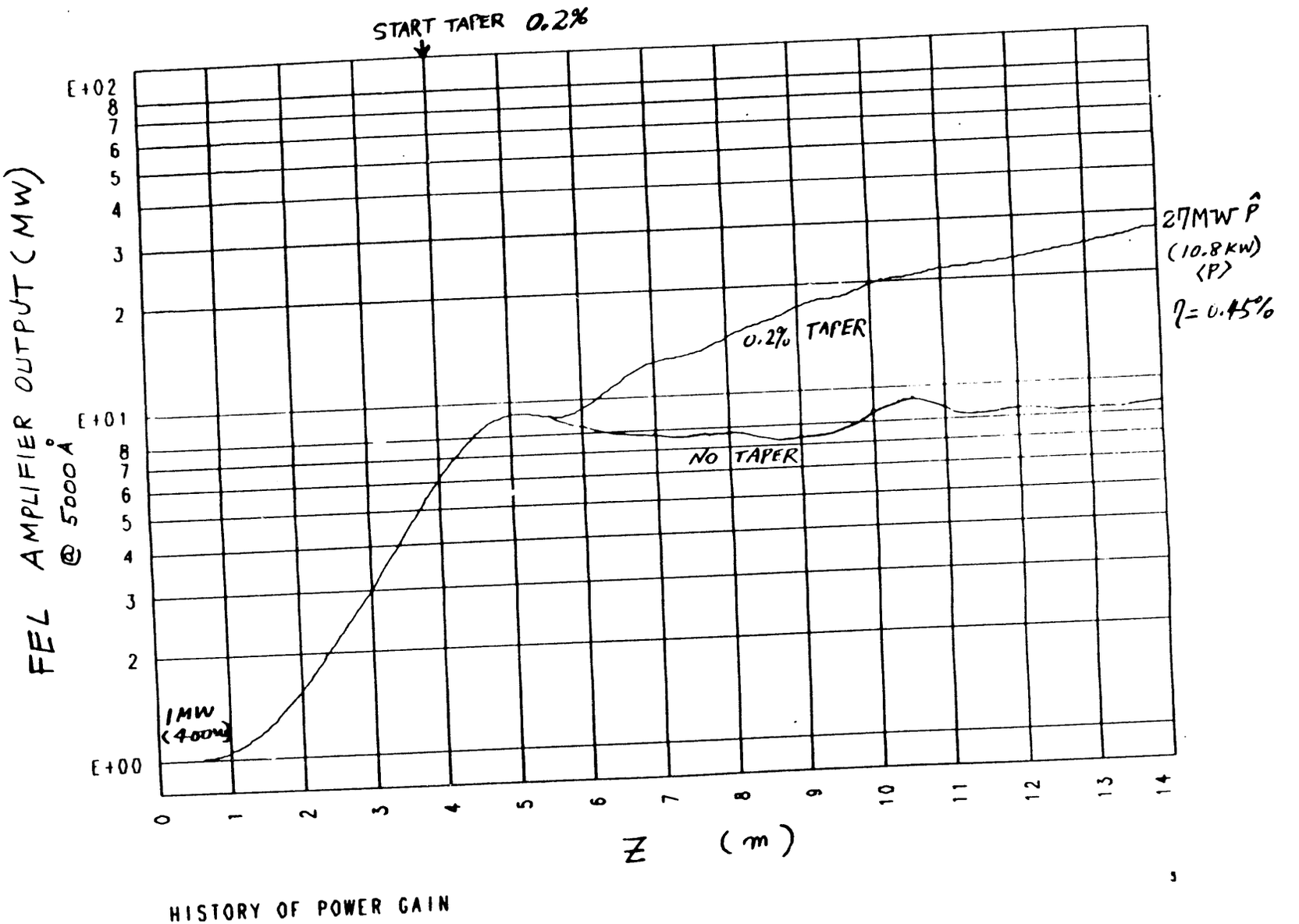

HISTORY OF POWER GAIN

Figure 13

efficiency is 0.45%. The case using an untapered wiggler is also shown for comparison.

In summary, with an FEL oscillator, an efficiency of 1.2% to 1.5% is feasible. However, the oscillator bandwidth must be investigated further. For the FEL amplifier, a very long wiggler is needed. In such a case, wiggler field errors may be a problem[28]. In both cases, further experimental and theoretical research would be useful.

5. References

1. L.R. Elias, W.M. Fairbanks, J.M.J. Madey, H.A. Schwettman, and T.I. Smith, Phys. Rev. Lett. **36**, 717 (1976).

2. C.W. Roberson and P. Sprangle, Phys. Fluids **B1**, 3 (1989).

3. T.C. Marshall, *Free Electron Lasers* (Macmillan, New York, 1985), p. 78.

4. IEEE J. Quantum Electrons, Special Issue on Free Electron Lasers, **QE–17**, p. 1326 (1981); **AE–19**, 256 (1983), **QE–21**, 804 (1985), **QE–23**, 1468 (1987).

5. M. Billardon, P. Elleaume, J.M. Ortega, C. Bazin, M. Bergher, M. Velghe, D.A.G. Deacon, and Y. Petroff, J. Quantum Electron, **QE–21**, 805 (1985).

6. J.A. Edighoffer, G.R. Neil, S. Fornaca, H.R. Thompson, T.I. Smith, H.A. Schwettman, C.E. Hess, J. Frisch, and R. Rohatgi, Appl. Phys. Lett **52**, 1569 (1988).

7. T.W. Meyer, R.L. Gullickson, B.J. Pierce, and D.R. Ponikvar, Nucl. Instrum. Methods (in press).

8. S. Penner, R. Ayres, R. Cutler, P. Bebenham, B.C. Johnson, E. Lindstrom, D. Hohr, J. Rose, M. Wilson, P. Sprangle, and C.M. Tang, Nucl. Instrum. Mehtods A **272**, 73 (1988).

9. R. Warren and J.C. Goldstein, Nucl. Instrum. Methods A **272**, 155 (1988).

10. D.A.G. Deacon, L.R. Elias, J.M.J. Madey, G.J. Ramian, H.A. Schwettman, and T.I. Smith, Phys. Rev. Lett. **38**, 892 (1977).

11. R.W. Warren, D.W. Feldman, J.E. Sollid, W.E. Stein, W.J. Johnson, A.H. Lumpkin, J.C. Goldstein, Report LA–U2–88–3586, to be published in Proc. 1988 FEL Conf., Nucl. Instr. and Methods A (1989).

12. T.F. Godlove and P. Sprangle, Naval Research Laboratory Report 6463, May, 1989.

13. T.P. Starke, IEEE Tans. Nucl. Sci. **Ns-30**, 1402 (1983).

14. D.C. Moir et al., IEEE Trans. Nucl. Sci. **NS-32**, 3018 (1985).

15. C.E. Hess, H.A. Schwettman and T.I. Smith, "Harmonically resonant cavities for high brightness beams," Proc. Particle Accelerator Conf., Vancouver, B.C. (published in IEEE Trans. Nucl. Sci.) (1985).

16. P. Elleaume, J.M. Ortega, M. Billardon, C. Bazin, M. Bergher, M. Velghe, and Y. Petroff, Jorunal de Physique, **45**, 989 (1984).

17. M. Billardon, P. Elleaume, Y. Lapierre, J.M. Ortega, C. Bazin, M. Bergher, J. Marilleau, and Y. Petroff, Nucl. Instr. & Methods in Phys. Res **A250**, 26 (1986).

18. G.A. Kornyukhin, G.N. Kulipanov, V.N. Litvinenko, N.A. Mesentsev, A.N. Skrinsky, N.A. Vinokurov and P.D. Voblyi, Nucl. Instr. & Methods in Phys. Res. **A237**, 281 (1985).

19. V.N. Litvinenko, "Storage ring FELs and its prospects," Twenfth Int. FEL Conf., Paris, (Nucl. Instr. Methods, to be published) (1990).

20. D.A.G. Deacon and J.M.J. Madey, Phys. Rev. Lett. **44**, 449 (1980).

21. W.B. Colson, Free Electron Lasers, Proc SPIE Vol. **738**, pages 2-27 (1987).

22. R.L. Tokar, B.D. McVey and J.C. Goldstein, IEEE J. Quantum Electron. **QE-24**, 856 (1988).

23. B.D. McVey, J.C. Goldstein, R.L. Tokar, C.J. Elliott, S.J. Gitomer, M.J. Schmitt and L.E. Thode, Nucl. Instr. Methods **A285**, 186 (1989).

24. T. Jeys, MIT Lincoln Laboratory, private communication.

25. T. Doering, W. Gallagher, R. Kennedy, B. Robinson, D. Shoffstall, E. Tyson, A. Vetter, and A. Yeremian, Nucl. Instr. & Methods in Phys Res. **A259**, 49 (1987).

26. W.M. Kroll, P.L. Morton and M.W. Rosenbluth, IEEE J. Quantum Electron., **QE-17**, 1436 (1981).

27. T.M. Tran and J.S. Wurtele, "Review of free-electron laser simulations techniques," Phys. Reports, Vol. 195, No. 1, (1990).

28. B.M. Kincail, J. Opt. Soc. Am., **B2**, 1294 (1985).

6. Publication and Reports

6.1 Publication

The abstract of a paper for the IEEE Lasers and Electro-Optics Society (LEOS) Annual Meeting in Boston was published during this time period. The paper was entitled "Design of a Narrow Bandwidth, Visible-Wavelength Free Electron Laser," by S.C. Chen, B.G. Danly, R.J. Temkin and J.S. Wurtele. The paper was accepted for the meeting and scheduled for oral presentation on November 8, 1990.

6.2 Reports

Progress reports were presented to MIT Lincoln Laboratory on November 9, 1989; February 8, 1990 and June 8, 1990. A presentation was also made at WSMR on December 1, 1989. Copies of the viewgraphs from these meeting are available.

Appendix 1:
Design of an Optical Wavelength FEL

Design of an Optical Wavelength FEL

R.J. Temkin
M.I.T.

August 10, 1989

This report was prepared for:
M.I.T. Lincoln Laboratory

Abstract

The design of an optical wavelength FEL is considered. The FEL is planned to operate with 7J of output power in 100 μs macropulses at 1 kHz repetition rate yielding 7 kW of average power. A number of FEL design options are considered; a detailed design is presented based on an RF linac operating at 120 MeV. An optical bandwidth of about 0.1 cm^{-1} is required, resulting in the selection of a 200 ps micropulse length. The micropulse separation is chosen to be 80 ns. It is proposed to multiply the repetition rate of optical micropulses external to the FEL cavity using a beamsplitter technique so as to reduce the micropulse spacing to 10 ns. The optical FEL has a design small signal gain of 10 to 20% and an efficiency of 1 to 2%. The resulting design is similar to the design of the Boeing, 0.5 μm wavelength FEL except for the micropulse length and a detailed comparison is presented. Although the proposed FEL design contains some novel features, the FEL appears feasible and capable of meeting the desired specifications.

1. FEL Optical Output Specification

The M.I.T. Lincoln Laboratory is currently investigating the feasibility of building an FEL (free electron laser) as a source of narrow bandwidth, one to ten kilowatt average power level radiation at visible wavelengths. The parameter range of interest is listed in Table 1. The average optical power is given as 7 kW in a train of 7J, 100 μs pulses at 1 kHz repetition rate. A special feature of the FEL design is the requirement of a narrow bandwidth, 0.1 cm^{-1} (3 GHz in frequency or 3 pm in wavelength). This will require micropulses of at least 333 ps duration in order to allow an optical bandwidth of 3 GHz to be achieved. Here, we are using the condition $(\Delta\nu)(\Delta t) \leq 1$ which is appropriate for the transform limited bandwidth of square (as opposed to Gaussian) pulses. If shorter micropulses are used, such as 200 ps, the transform limited bandwidth would increase to about 5 GHz. A shorter micropulse length such as 200 ps might be acceptable if the energy per pulse is increased appropriately, so that about 7J is available in a 0.1 cm^{-1} bandwidth. Thus, for a 200 ps micropulse, the required energy per macropulse should increase by (5 GHz/3 GHz) to 11.7J.

In practice, it may not be possible to achieve transform limited output pulses from an FEL. However, it is necessary to be within about a factor of two of such transform limited operation in order to achieve adequate output power. For an FEL oscillator, wide bandwidth emission may occur due to sideband generation. Power appearing in sidebands is undesirable. For these specifications, we will consider power in sidebands to be a problem only in so far as it reduces the output power in the 0.1 cm^{-1} wide central frequency region of interest. Power in sidebands can be filtered from the optical beam using gratings, for example.

2. Concepts for a Visible Wavelength FEL

A. FEL Accelerator Options

Free electron lasers have operated at visible wavelengths in several laboratories and using several different accelerators. The first operation of an FEL at visible wavelengths was achieved on the ACO storage ring at Orsay, France. The ACO storage ring FEL has 0.5 ns micropulses with 37 ns spacing between micropulses. The relatively long micropulses are attractive for the present application. However, the output power of the storage ring FEL is limited by the need to recirculate the electron beam. Storage ring FEL operation to date is not consistent with kW average power level operation in the visible regime. Methods of

Table 1
Optical FEL Specifications

Wavelength:	$\lambda = 500$ to 600 nm
Pulse Length: (Macropulse)	$\tau_{MP} = 100\mu s$
Pulse Energy: (Macropulse)	$E_{MP} = 7J$
Repetition Rate: (Macropulse)	1 kHz
Laser Bandwidth:	$\Delta\nu \leq 0.1$ cm^{-1}
Laser Power, Macropulse Average	70 kW
Laser Power, Time Average	7 kW
Micropulse Separation	$\leq$ 10 ns

increasing the output power of a storage ring FEL may merit further analysis. Storage rings are also being developed for x-ray lithography applications using synchrotron radiation. A possible dual use facility, as an FEL and lithography system, might be attractive.

Visible wavelength emission has been achieved with a conventional RF linear accelerator at Boeing and with a superconducting accelerator at Stanford. The Boeing device is relatively close to the present optical FEL specifications, with a design of 30 kW of macropulse average power at 0.5 μm wavelength. A major difference between the Boeing FEL and the present design is that the Boeing FEL has a 16 to 20 ps micropulse length vs. 200 ps in the present design. A design of an optical FEL with a 200 ps micropulse length is presented in the next section and compared with the Boeing FEL parameters. A superconducting FEL might also prove attractive for a visible wavelength FEL. At present, superconducting accelerator technology is less well developed than conventional (copper) accelerator technology. Hence, superconducting accelerators will not be considered in detail.

Other approaches for a visible wavelength FEL have also been suggested. A near infrared FEL was built by J. Madey and coworkers at Stanford and the FEL output was converted to visible radiation by doubling twice in nonlinear crystals outside of the FEL. This may not be practical for kW average power levels. The FEL itself can also generate harmonics, particularly the third harmonic, but such harmonic operation is not adequately demonstrated at present. The use of electrostatic accelerators, which operate at moderate voltages, and a very short period wiggler has been proposed for an optical FEL but has not been demonstrated. An induction linac FEL can operate at visible wavelengths but the pulse length is 50 ns, much shorter than the desired 100 μs. Also, the accelerator size is large and is inconsistent with kW power level operation.

For these reasons, an RF linac has been selected for a first FEL design.

B. RF Linac with Long Micropulses

The micropulse length must be of order 200 ps or greater in order to achieve a narrow FEL emission bandwidth. This micropulse length is an order of magnitude longer than the state of the art. Present day accelerators operate with micropulse lengths of 3 to 20 ps. Several concepts are promising for generating long micropulses from an RF linac but all are somewhat risky. A very high beam quality must be achieved in all cases. This beam quality requirement may be difficult to achieve.

A conventional RF accelerator, producing 20 ps pulses, could be cnstructed and followed by a pulse stretcher. The pulse stretcher would be a lengthy beam line or ring. Stretching might be achieved passively using magnetic fields and the inherent small energy spread in the beam. Stretching might also be achieved actively using RF cavities to spread out the beam.

A novel accelerator capable of accelerating long micropulses has been designed by Hess, Smith and Schwettman of Stanford. The accelerator uses cavities fed with both a fundamental and a harmonic frequency to accelerate long micropulses. A design for 200 ps micropulses was reported but has not been tried.

A very low frequency accelerator, operating at a frequency of about 80 MHz, or less, could produce 200 ps micropulses. This accelerator frequency is about five to fifteen times lower than present day values, thus allowing the factor of ten increase in micropulse length. Low frequency electron accelerators are larger and longer than higher frequency accelerators, increasing cost. A 50 MHz electron accelerator has been operated at Los Alamos, but the beam quality was not very good.

The above options need further investigation. The use of a 20 ps micropulse accelerator with a stretcher would allow an early test of the concepts proposed here. The stretcher could be added to a present day FEL such as the Boeing device. This would greatly reduce the cost of a proof–of–principle experiment.

3. Optical FEL Design

A. FEL Design Parameters

The design parameters of an optical FEL with the specifications listed in Table 1 are presented in Tables 2 and 3. The design of an FEL is influenced heavily by the need to have excellent electron beam quality from the accelerator and the need to have high gain in the optical resonator. The design presented in Tables 2 and 3 is optimized with respect to these basic design constraints.

Many of the design parameters in Tables 2 and 3 are directly consistent with modern FEL technology. Using a conventional wiggler period of 2 cm, a beam energy of 120 MeV is needed. A wiggler field producing an a_w of 1.33 is assumed so as to achieve high gain. These numbers are very similar to the Boeing FEL design.

Some novel features of the present design arise from the need for a 200 ps (or greater) micropulse, combined with the need for good beam quality, kilowatts of average power and an optical gain exceeding 10%. The gain of the FEL increases approximately linearly with current, so high peak currents are desirable. However, the use of high currents, of order 100 A, would result in too high an average output power if an efficiency of 1% is achieved. A peak current of 25 A has been selected yielding micropulses with a 5nC charge. This charge is consistent with high power accelerator designs at Los Alamos. To maintain an average output power of 7 kW, the micropulse separation has been increased to 80 ns, which is larger than the 10 ns specified in Table 1. It is proposed to build an optical pulse multiplier outside of the FEL to produce the 10 ns pulse separation specified in Table 1. This is described in another section.

The design in Tables 2 and 3 yields a small signal gain of 20% per pass excluding gain reduction due to beam quality effects. The most serious beam quality problem may be energy spread. A 1% energy spread will reduce the gain by about a factor of two. Computer calculations of FEL gain would be useful to verify that the gain exceeds 10%. There is some uncertainty in the FEL gain due to the uncertainty in the electron beam quality that can be achieved.

Table 2
Wiggler and Resonator Parameters

Wiggler Period:	$\lambda_w = 2.0$ cm
Wiggler Length:	Uniform Length, 1m (50 periods) Tapered Length, 1m (50 periods) Total Length, 2m (100 periods)
Magnetic Wiggler Field:	$B_0 = 1.0$ T
Magnetic Gap:	4 mm (approx.)
Normalized Vector Potential:	$a_w = 1.33$
Betatron Wavenumber:	$k_\beta = a_w k_w/\sqrt{2}\gamma = 1.22 \times 10^{-2}\text{cm}^{-1}$
Betatron Period:	$L_\beta = 2\pi/k_\beta = 5.1\text{m}$
Optical Beam Waist:	$w_0 = 0.4\text{mm}$
Rayleigh Range:	$Z_R = \pi w_0^2/\lambda = 1\text{m}$
FEL Output Efficiency	$\eta = 1/2N = 0.01$
FEL Small Signal Gain per Pass:	$G = 10 - 20\%$

Table 3
Optical FEL Accelerator Parameters

Electron Beam Energy: (For $\lambda = 0.5\mu$m)	$U = 120$ MeV $\gamma = 236$
Energy Spread, full width	$\Delta\gamma \mid \gamma < 1\%$
Peak Electron Beam Current:	$I = 25$A
Peak Electron Beam Power:	3 GW
Micropulse length:	200 ps
Charge per micropulse:	5 nC
Micropulse separation:	80 ns
Macropulse length:	100 μs
Macropulse repetition rate:	1 kHz
Electron beam brightness:	$B_N = 370$ kA/cm^{2}rad^2
Electron beam emittance:	$\varepsilon_N = 50$ mm mrad
Electron beam radius:	$r_{eo} = 0.40$ mm
Macropulse average electron current:	63 mA
Macropulse average electron beam power:	7.5 MW

An FEL efficiency of about 1% is projected. With a tapered wiggler, an efficiency closer to 2% may be possible, in theory. The time average output power is 7.5 kW at 1% efficiency or 15 kW at 2% efficiency. The output power should exceed 11.7 kW in a 200 ps, transorm-limited pulse in order to meet the 7 kW in 0.1 cm^{-1} bandwidth specification of Table 1.

B. Optical Pulse Repetition Rate Multiplier

The FEL design in Tables 2 and 3 requires an 80 ns micropulse separation in order to meet peak and average power requirements. A method for dividing and splicing picosecond pulses in order to increase the repetition rate has been reported by A. Mooradian of M.I.T. Lincoln Laboratory, (Applied Physics Letters **45**, 494, 1984) and is shown in Figure 1. The technique uses beam splitters and delay lines to divide and recombine the optical beam. This technique may be feasible at kilowatt power levels. The purpose of the multiplier is to change the micropulse spacing from 80 ns to 10 ns. The output of the multiplier consists of two optical beams. These can possibly be combined using a polarizing beam splitter. Alternate concepts for pulse frequency multiplication may also be feasible.

The use of a micropulse spacing of 80 ns in the FEL produces an increase in FEL gain by a factor of eight relative to the same FEL with a 10 ns spacing. This increase in gain appears to be critical in obtaining good FEL performance. Therefore, the optical pulse multiplier is a necessary component in the proposed optical FEL design.

C. Comparison with Boeing FEL

The present design of an optical FEL is based on optimizing the FEL gain and efficiency for the specified peak and average output powers. However, the resulting design is rather similar to the published design of the Boeing visible wavelength FEL. A comparison of the two designs is given in Table 4. The Boeing FEL is designed for higher extraction efficiency, 5%, vs. the 1 to 2% of the present design. The peak current and peak optical power are higher in the Boeing design. However, the present design has a higher optical output power when averaged over a macropulse.

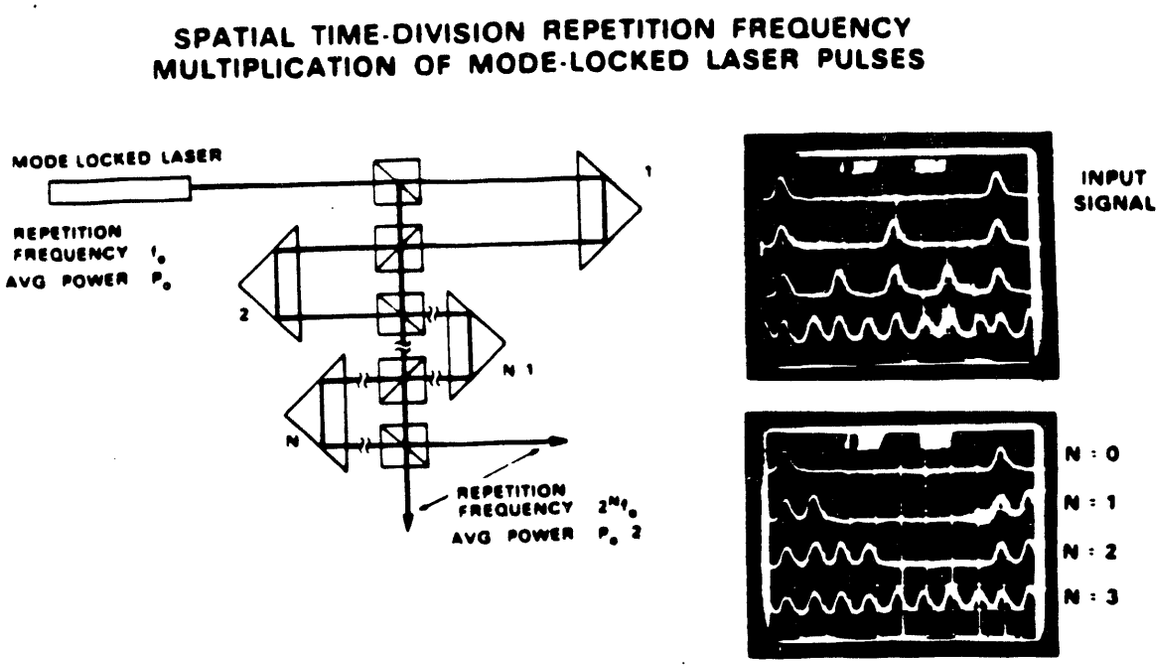

Figure 1: Pulse Repetition Rate Multiplication Concept

Table 4
Boeing FEL vs. Optical FEL Design

	Boeing	Optical FEL
λ	514 nm	500–600 nm
λ_w	2.18 cm	2 cm
Beam energy	123 MeV	120 MeV
Energy Spread	1%	1%
Wiggler, Uniform region length	0.88 m	1.0 m
a_w	1.33	1.33
Betatron Wavelength	5.6 m	5.1 m
Optical beam waist	0.6 mm	0.4 mm
Rayleigh Range	2.4 m	1.0 m
Electron beam radius	0.35 mm	0.4 mm
Micropulse Length	20 ps	200 ps
Micropulse Separation	28/250 ns	80 ns
Peak Current	100 A (250 A)	25 A
Macropulse length	100 μs	100μs
Beam emittance	33 mm mrad	50 mm mrad
Micropulse peak optical power	600 MW	30 MW
Macropulse average optical power	30 kW	70 kW
Optical extraction efficiency	5%	1%
Small signal gain	20%	10–20%
Startup time	60 μs	12–24 μs

4. Discussion and Conclusions

An optical wavelength FEL producing narrow bandwidth output pulses at kilowatts of average power has been considered. A specific design has been developed and compared with the Boeing FEL. The resulting design appears feasible. However, some aspects of the design depend on undemonstrated or possibly risky technology. We do not know whether an accelerator with 200 ps pulses and excellent beam quality can be developed. The FEL is designed to operate at greater than 1% extraction efficiency in a nearly transform-limited optical mode. The 10 μm wavelength FEL at Los Alamos has been operated with high efficiency, up to 4%. It has also shown good optical quality with suppression of sidebands. These results have not been demonstrated yet, to my knowledge, at visible wavelengths. FEL operation at visible wavelengths requires much higher beam energy than at 10 μm, 120 MeV vs. 20 MeV. This results in a more stringent requirement on the accelerator design. The present optical FEL requires a 1 kHz repetition rate which is also not demonstrated for a high power accelerator or FEL. However, Boeing is planning an accelerator test at 10 MeV and 1 A of average current, which is an order of magnitude higher in beam power than the proposed design.

The present FEL design is based on linear FEL theory with first order corrections for beam qualtiy. A better design with an optimized gain could be obtained using available FEL codes.

Other issues include the damage to the optics arising from spontaneous emission from the electron beam passing through the wiggler. The optical output power might also lead to damage due to the small optical spot size. The concept of a micropulse frequency multiplier needs to be demonstrated at high power.

The design of a 200 ps accelerator or pulse stretcher needs some investigation. The required charge in each micropulse is relatively high raising additional questions regarding feasibility of the accelerator design and possible beam breakup instabilities.

The present design of an optical FEL contains several novel features. Nevertheless, the basic design parameters appear to be feasible. The beam quality requirements are stringent but not different from those of other FEL devices. The average optical power of about 10 kW makes the FEL a very useful device. In all, I believe that the proposed FEL is feasible.

END

DATE FILMED

12/05/91